Asian Journal of Chemistry; Vol. 34, No. 11 (2022), 2771-2785

ASIAN JOURNAL OF CHEMISTRY

https://doi.org/10.14233/ajchem.2022.23863

REVIEW

Structurally Characterized Non-Heme Fe(IV)Oxo Complexes: A Brief Overview

JHUMPA MUKHERJEE[1,*] and SRIPARNA RAY[2]

[1]Department of Chemistry, Dum Dum Motijheel College, Dum Dum, Kolkata-700074, India
[2]Department of Chemistry, School of Basic Sciences, Faculty of Science, Manipal University Jaipur, Dehmi Kalan, Jaipur-303007, India

*Corresponding author: E-mail: jmukherjeeddmc@gmail.com

Received: 7 April 2022; *Accepted*: 22 June 2022; *Published online*: 19 October 2022; AJC-20986

Iron(II) centers found in both heme and non-heme enzymes, are the most important metal centre responsible for effectively activating molecular oxygen. Activation of molecular oxygen is important for natural systems and many industrially important reactions. Iron(IV)oxo unit is one of the important intermediates found among the various high valent oxo iron intermediates formed during substrate oxidation in natural enzymes. In this review article, the different synthetic strategies were focused and followed to obtain the X-ray structurally characterized model iron(IV)oxo complexes with non-heme ligands. The ligands were categorized in three different classes and showed how designing a proper ligand, binding with Fe(II) center and reacting it with a suitable oxidizing agent can finally give rise to a system similar to natural systems. Stability of these complexes and some preliminary characterization have also been discussed. The crystallographic characterization of these synthetic models containing iron(IV)oxo intermediates was necessary to understand the mechanistic pathway they follow to mimic the difficult oxidation reactions performed by natural enzymes. In this review, not only the synthetic strategies for these non-heme iron(IV)oxo complexes were highlighted but a detailed structural analysis for these important intermediates were also discussed.

Keywords: Iron(IV)oxo, Non-heme, Synthetic model, X-ray structural parameters.

INTRODUCTION

Iron is one of the transition elements frequently found at the active site of many proteins and enzymes, hence these constitute an important class of biologically active compounds. The diverse biological functions of iron containing proteins/enzymes include hydroxylations, O-atom transfers, halogenation, desaturation, cyclization, epoxidation and decarboxylation [1-7]. In nature, dioxygen is an abundant and potentially powerful oxidizing or oxygenation agent for organic compounds. While reactions of oxygen with organic compounds are thermodynamically favourable, they tend to be kinetically unfavourable due to its triplet ground state. Additionally, reduction of O_2 by single electron to form a superoxide is also unfavourable. In contrast, the reactions involving an overall four-electron reduction of O_2 to water or a two-electron reduction to peroxide are thermodynamically favourable [8]. In fact, the most common pathway for dioxygen activation, which engages O-O bond cleavage, is carried out *via* the mediation of a transition metal ion. The greater spin-orbit coupling in metal ions reduces the kinetic barrier of dioxygen activation, thereby facilitating the chemical transformation. Coordination with a metal center not only makes the one-electron reduction of O_2 easier, but also helps to access the two and four-electron reduction pathways [9-13].

In many biological oxidation processes, high valent metal-oxo complexes of Fe, Mn, Cu are present as intermediates. Iron is one of the first row transition metals, which is found in a variety of metalloenzymes, because it is abundantly available, have an extensive redox chemistry and can readily bind to dioxygen. In addition, various spin states are available for the different common oxidation states of iron. Thus, it has been observed that high spin iron(II) is the most important metal center utilized for activation of molecular oxygen. After binding with oxygen, homolytic or heterolytic O-O bond cleavage helps in substrate oxygenation. Mechanism proposed for these oxyg-

enation reactions, for both heme and non-heme enzymes, involve various high-valent oxo iron intermediates. In many studies, these intermediates are trapped and in-depth spectroscopic studies and computational analysis have been done. In this context, it is noteworthy that iron-based enzymes can be categorized with respect to the number of iron centers within them, specifically, mononuclear *e.g.*, Cyt P450 and dinuclear, *e.g.*, methane monooxygenase (MMO). Depending on the ligand environment, they could be classified as heme or non-heme type enzymes (Fig. 1). In heme proteins or enzymes, a Fe(II) active site is bound to a porphyrin macrocycle, whereas in non-heme, a triad of ligands, such as, two histidiene, one monodentate carboxylate and two to three water ligands are bound in most cases [14]. Crystal structures are available for many of these enzymes [15-23]. A notable fact is that the heme sites are rigid and only one vacant site is available to bind the molecular oxygen. In contrast, non-heme sites are more flexible, they have more exchangeable sites for binding of substrate and cofactor. Additionally, each of these classes can consist of different varieties of enzymes on the basis of their catalytic ability, *e.g.*, monooxygenases and dioxygenases. In different mononuclear iron containing heme enzymes like peroxidase, catalase and oxygenase, an active iron(IV)oxo porphyrin radical cation intermediate called compound **I** is formed [24-30]. In mononuclear non-heme enzymes, the active site could be Fe(III) [*e.g.* intradiol dioxygenases and lipoxygenases] or Fe(II) [*e.g.* Taurine α-KG dioxygenase (Tau D), cysteine dioxygenase, α-ketoglutarate-dependent prolyl hydroxylase, bleomycin, phenylalanine hydroxylase] [31-34]. Two very different types of intermediates could be formed, either, an iron(III) coordinated with superoxo (O^{2-}) [*e.g.* isopenicillin-N synthase (IPNS)] or high-valent Fe(IV)oxo [*e.g.* Tau D] [5,20]. For mononuclear non-heme, as in Rieske dioxygenases, an Fe(V)oxo intermediate is accepted to be responsible for substrate oxidation. The ligands, attached to the Fe center, have less covalent interaction compared to heme units and this affects the active site by influencing the mode of binding of O_2 [35]. Characterization of these non-heme Fe centers are quite difficult, due to lack of any intense band in the absorption spectroscopy. Additionally, the conventional EPR spectrum cannot be recorded for Fe(II) ($3d^6$), high spin (s = 2) centers.

Interests in elucidating or mimicking the physico-chemical properties of these iron containing metalloproteins led to the synthesis of numerous interesting coordination complexes containing iron as the active center. The complexity of biological systems renders a detailed study of their mechanism very difficult. A simple chemical compound or system, designed using inexpensive and readily available transition metal center, can be used as functional and structural model of these metalloproteins. These catalysts synthesized in the laboratory could be further used for oxidation of many organic substrates, rendering them useful in different chemical and pharmaceutical industries.

Ligand selection for Fe(IV)oxo complexes: Monooxygenation of the aliphatic C-H bonds of various substrates can be effectively catalyzed by the cytochrome P450 enzyme, which consists of a heme cofactor. Various research groups have been investigating different biomimetic complexes, which are either the structural models or the functional ones of this enzyme system. The ultimate aim is to understand the mechanism involved by the iron centers, while activating dioxygen and the consequent oxidation of the substrates. In most cases, the octahedral Fe-center in the heme cofactor is coordinated to a porphyrin ring at the equatorial positions and two other axial ligands are also present. Hence, researchers have involved various tetradentate and pentadentate non-heme ligand systems to explore and mimic the catalytic system of the P450s. While choosing the non-heme ligand systems, various criteria were involved. First, the catalytic ability of non-heme Fe complexes to facilitate alkane hydroxylation was explored. Secondly, the reaction intermediates of the catalytic cycles, especially, the iron peroxo and Fe(IV)oxo intermediates, were investigated to correlate with the proposed mechanisms involving monooxygenases. Additionally, electronic properties of the iron complexes were tuned to mimic those of the P450 systems. Hence, in order to avoid the complexities caused by the porphyrin system, two non-heme ligand frameworks were widely

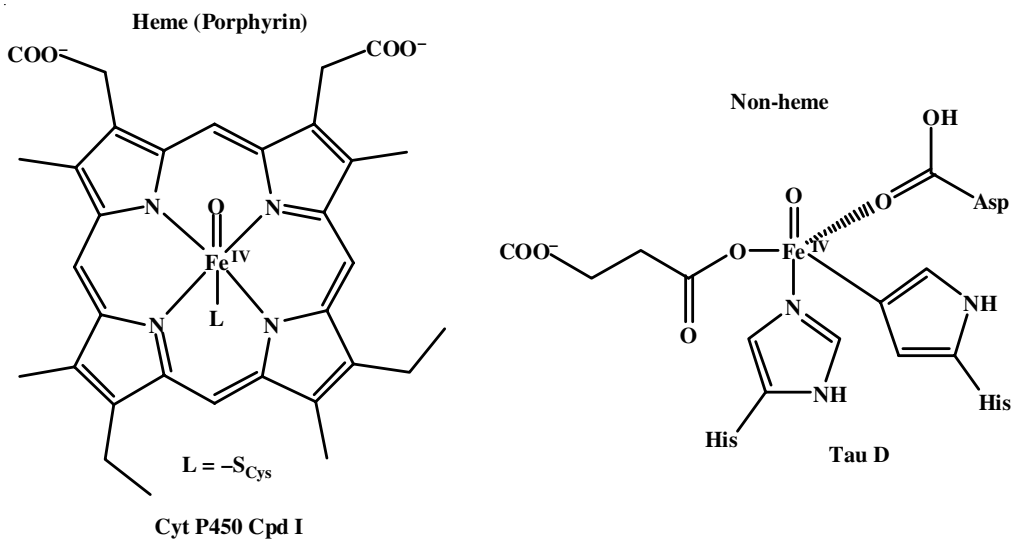

Fig. 1. Example of heme and non-heme type enzymes containing Fe(IV)oxo unit

explored, one being tetradentate and the other being pentadentate. Another prominent feature was that non-heme systems containing 3 or more N-donors were extensively studied, which were apparently similar to the N-donors of the heme-porphyrin systems. Moreover, being strong s donors, these ligand frameworks were able to facilitate the stabilization of Fe(IV) oxidation state in the complexes. One of the initial ligands, *tris*(2-pyridylmethyl)amine (TPA) ligand, which is tetradentate and its iron complex acted as a functional mimic of monooxygenases [36]. Through spectroscopic and reactivity studies, it was proved that it could effectively mimic the dinuclear non-heme iron enzymes, as in methane monooxygenase.

Based on the nature of coordination and the donor atoms involved, the non-heme ligand frameworks, discussed in this review, can be loosely classified into the following broad categories: the macrocyclic cyclam based ones, the pentadentate N4Py or N2Py2X variety, tripodal N4 ligands and the macrocyclic tetracarbene based ligand. The cyclam or 1,4,8,11-tetraazacyclotetradecane framework is one of the successful candidates to coordinate to the iron center and form the biomimetic complexes (Fig. 2A). In fact, the first spectroscopic evidence of a mononuclear Fe(IV)oxo species is reported by Grapperhaus *et al.* [37] using 1-carboxymethyl-1,4,8,11-tetraazacyclotetradecane as the tetradentate ligand and a tetramethylated cyclam was effectively utilized by Que *et al.* [38] to produce the high resolution crystal structure of the Fe(IV)oxo species. Here, 1,4,8,11-tetramethyl-1,4,8,11-tetraazacyclotetradecane ligand (**1**), being tetradentate, the fifth coordination site of Fe(IV) was occupied by CH_3CN solvent. The ligand can be synthesized, following the Barefield & Wagner's procedure [39], by the methylation of 1,4,8,11-tetraazacyclotetradecane by refluxing the tetramine with commercially available formic acid (98-100%) and formaldehyde (40%) in water for 24 h [38]. After appropriate workup, 1,4,8,11-tetramethyl-1,4,8,11-tetraazacyclotetradecane can be obtained as long colourless needles.

Belonging to the same category of cyclam ligands, two pentadentate 1,4,8,11-tetraazacyclotetradecane ligands with suitable pendant arms have also been synthesized and their iron complexes were explored as non-heme mononuclear iron enzyme mimics. The joint efforts of Münck and other groups [38,40-44] led to the report of a structurally characterized Fe(IV)oxo complexed by a pentadentate ligand (**2**) (Fig. 2B). In order to closely resemble the electronic environment around a Fe(IV)oxo complex in a monooxygenase enzyme, the authors sought to mimic the presence of the imidazole moiety in the *trans*-position to the Fe(IV)oxo. This coordination was expected to facilitate the formation and stability of high valent Fe(IV)oxo intermediate. Hence, 2-pyridylmethyl arm was appended to the cyclam framework and subsequent formation of the Fe(IV)-oxo species was studied with this pentadentate ligand (**2**). The 1,4,8-trimethyl-1,4,8,11-tetraazacyclotetradecane [45], was utilized to synthesize the cyclam macrocycle containing the pendant pyridyl arm. The trimethylcyclam was reacted with equivalent amount of picolyl chloride, in presence of eight equivalents of base [40]. Thereafter, following appropriate workup, produced the pentadentate ligand as a yellow oil in excellent yields. On complexing with Fe(II) ion, the pyridyl moiety was observed to be positioned at the apical part of a distorted square pyramidal complex.

In order to modulate the 2-His-1-carboxylate facial triad as is observed in a variety of enzymes, for example, TauD, the pentadentate cyclam ligand bearing an O-atom donor was utilized to synthesize and structurally characterize an ultrastable Fe(IV)oxo complex by Münck and Que groups [38,40-44]. Alkylating 1,4,8-trimethyl-1,4,8,11-tetraazacyclotetradecane with 2-chloro-*N,N′*-dimethylacetamide produced the macrocyclic cyclam ligand with *N,N*-dimethylacetamido donor (**3**) (Fig. 2C) [46].

The second category of ligands, which were successfully utilized for obtaining the Fe(IV)oxo complexes, are the pentadentate N4Py or N2Py2X variety, where X can be pyridine (Py), quinoline (Q), benzimidazole (B), *etc.* Que *et al.* [38,40-44] observed that instead of a tetradentate ligand, the Fe(IV)oxo moiety can be generated and better stabilized, with respect to thermal stability, by a pentadentate N5 ligand, for example, *N,N-bis*(2-pyridylmethyl)-*N-bis*(2-pyridyl)methyl-amine (N4Py) (**4**) (Fig. 3A). In fact, they were able to obtain high resolution X-ray diffraction crystals with this ligand for the Fe(IV)oxo species in 2005 [41]. Previously, they had even reported the catalytic efficiency of this complex for hydroxylating the alkyl C-H bonds [42]. N4Py was synthesized by reacting *bis*(2-pyridyl)methylamine with an alkaline solution of picolyl chloride hydrochloride in the ratio of 1:2, at room temperature [43]. This ligand was then utilized to produce the iron complex and its Fe(IV)oxo species was stable at room temperature, with a half-life of ~ 60 h. Another ligand family

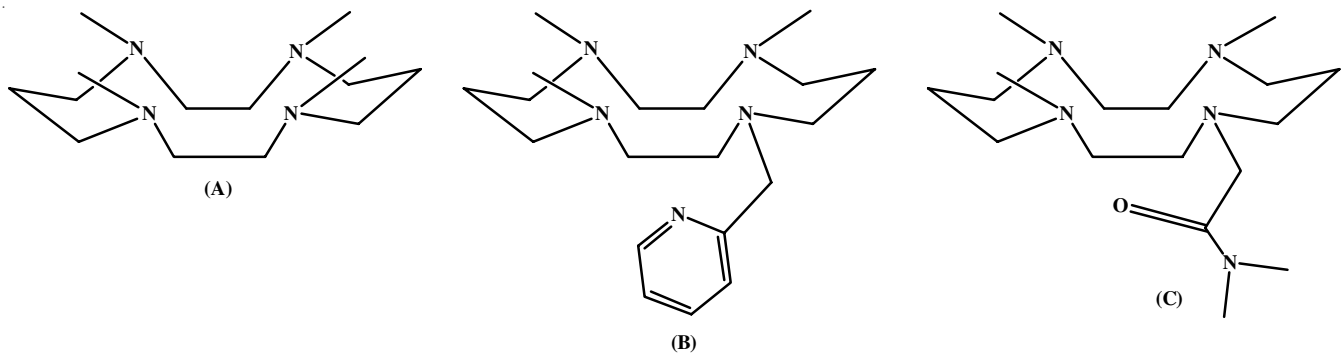

Fig. 2. (A) Cyclam or 1,4,8,11-tetraazacyclotetradecane (TMC) (**1**), (B) 2-pyridylmethyl substituted cyclam (TMC-py) (**2**), (C) *N,N*-dimethylacetamido substituted cyclam (TMC-dma) (**3**)

belonging to the pentadentate category was designed and synthesized by the Goldberg group [47], namely, $N4Py_2^{2ArF}$ (**5**), where ArF_2 = 2,6-difluorophenyl (Fig. 3B). Out of the various Fe(IV)-oxo complexes obtained from this class of ligands, they had structurally characterized the Fe(IV)oxo complex with the $N4Py_2^{2ArF}$ ligand in 2016 [48]. The initial step of the ligand synthesis involves a Suzuki cross-coupling reaction between *bis*(6-bromopyridin-2-yl)methanone and 2,6-difluorophenyl boronic acid in presence of XPhos-Pd-G2 catalyst to produce *bis*(6-(2,6-difluorophenyl)pyridin-2-yl)methanone, as a yellow solid. It was further reacted with hydroxylamine hydrochloride and sodium acetate, to form the corresponding oxime. Subsequently, it was reduced with Zn dust in alkaline conditions to produce the desired brown solid, *bis*(6-(2,6-difluorophenyl)-pyridin-2-yl)methanamine. The final reaction occurred in the presence of a strong base between *bis*(6-(2,6-difluorophenyl)-pyridin-2-yl)methanamine and 2-bromomethylpyridine hydrobromide and produced the $N4Py_2^{2ArF}$ ligand as a yellow solid.

In 2015, Nordlander *et al*. [49] suggested that the reactivity of Fe(IV)oxo complexes can be modified by tuning the steric and electronic properties of ligand framework, while keeping the thermal stability of the complexes intact. Hence, they derivatized the N4Py system by replacing the (2-pyridyl)methyl arms with other analogues of histidine moieties, for example, with (N-methyl)benzimidazolyl (**6**) or with quinolyl arms (**7**) (Fig. 3C-D), so as to retain the coordination of the N-atoms onto the Fe-center. The replacement of the pyridine moieties affected the steric bulk as well as the s-donation properties of the ligands. Thus, among the N2Py2X variety, two different ligands were synthesized and their Fe(IV)oxo complexes were structurally characterized by Que *et al*. in 2018 [50]. The N2Py2Q ligand was synthesized through the reaction of *bis*(2-pyridyl)methylamine with two equivalents of 2-(chloromethyl)quinoline hydrochloride, in presence of a base to produce a grayish yellow solid ligand. The N2Py2B ligand was synthesized using by reported method of Nordlander *et al*. [49]. They had reacted two equivalents of 2-chloromethyl-1-methylbenzimidazole with *bis*(2-pyridyl)-methylamine in presence of 5 M NaOH at room temperature for 3 days to obtain a sticky solid, which after appro-priate work-up produced the pale brown solid ligand. Both N2Py2B and N2Py2Q were utilized to synthesize the Fe(II) complex and Fe(IV)oxo complexes were obtained by reacting them with ceric ammonium nitrate (CAN).

A different category of ligand framework, consisting of tripodal N4 ligands, commonly known as 1,1,1-*tris*{2-[N2-(1,1,3,3-tetramethylguanidino)]ethyl}amine TMG_3tren, was first synthesized by Sundermeyer *et al*. [51] (Fig. 4A) [52]. The deuterated and peralkylated oligoguanidine, $TMG_3tren\text{-}d_{36}$ (**8**) was synthesized by Roth *et al*. [52] in 2007, which was further utilized by England *et al.* [44] in 2010 to synthesize and structurally characterize the Fe(IV)oxo complex. Phosgene was reacted with tetramethylurea-d_{12} to produce chlorotetramethyl-formamidinium chloride-d_{12}. This $[(Me_2N)_2CCl]Cl\text{-}d_{12}$ was futher reacted with perdeutero-*tris*(2-aminoethyl)amine, in presence of three equivalents of triethylamine. Deprotonation of the formerly obtained product led to the synthesis of the peralkylated oligoguanidine-d_{36}, as colourless crystals.

Prior to this, Holm *et al*. [53] and Lu & Valentine [54] in had reviewed on how ligands can be modified in order to modulate the electronic properties of the metal complex formed with

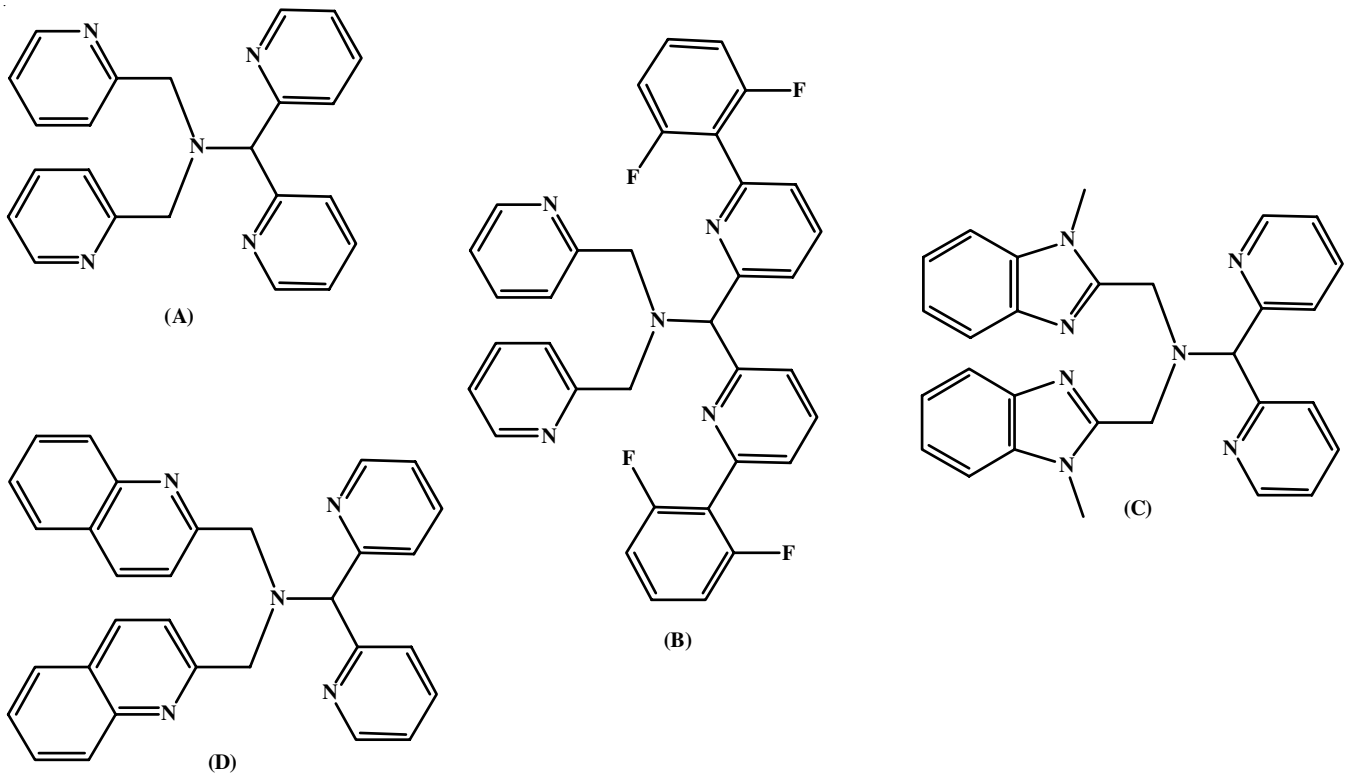

Fig. 3. (A) *N,N-bis*(2-pyridylmethyl)-N-*bis*(2-pyridyl)methylamine (N4Py) (**4**), (B) $N4Py^{2ArF_2}$ (**5**), where ArF_2 = –2,6-difluorophenyl (C) N2Py2B (**6**), where B = benzimidazole, (D) N2Py2Q (**7**), where Q = quinoline

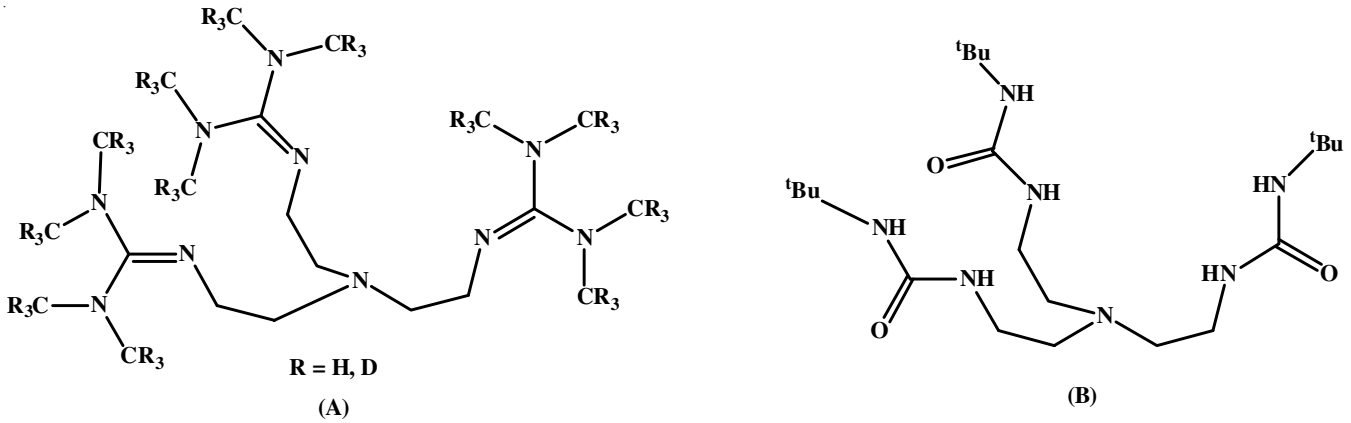

Fig. 4. (A) 1,1,1-*tris*{2-[N2-(1,1,3,3-tetramethylguanidino)]ethyl}amine ($TMG_3tren/TMG_3tren\text{-}d_{36}$)(**8**), (B) *tris*[(N'-*tert*-butylureayl)-N-ethyl]amine [(N-*tert*-butylureay1ato)-N-ethyl)]aminato ligand (**9**)

it and two N4 tripodal ligands were designed (Fig. 4B). In this respect, the ligand was designed to possess less steric bulk, greater s-donation properties as well as provide a cavity structure, which can accommodate intramolecular hydrogen bonding and stabilize the metal complex. The most interesting feature of this type of ligand is the fact there can be upto three H-bonds formed between the external donor atom to the metal center and the hydrogens present in this ligand. The importance of such hydrogen bonding is a well-recognized fact in various properties of metalloproteins. The active site as well as the catalytic properties of the metalloproteins can be regulated by channelizing the hydrogen bonds along with the bonds formed between the metal center and the donor atoms of the ligand. Hence, *tris*[(*N*-*tert*-butylureay1ato)-*N*-ethyl)]-aminato ligand (**9**) was synthesized following the reported synthetic procedure of a similar ligand (Fig. 4B) [55]. *Tris*(2-aminoethyl)amine was reacted with three equivalents of *tert*-butyl isocyanate to produce the required tripodal *tris*(ureaylato) ligand, which could successfully stabilize the Fe(IV)oxo species.

A very different type of macrocyclic ligand, $[(L^{NHC})H_4](OTf)_4$, 3,9,14,20-tetraaza1,6,12,17-tetraazoniapentacyclohexacosane-1(23),4,6(26),10,12(25),15,17(24),21-octaene *tetrakis*-trifluoromethanesulfonate, based on *N*-heterocyclic carbene (NHC) was utilized by Meyer *et al*. [56] to synthesize the Fe(IV)oxo complex (Fig. 5). The 18-Atom-ringed macrocyclic ligand was initially reported by Bass *et al.* in 2010 [57]. The 1,1′-methylene(*bis*imidazole) was synthesized by reacting two equivalents of imidazole with dichloromethane in presence of four equivalents of KOH and a phase transfer catalyst, *tert*-butyl ammonium bromide (TBAB) [58]. The *bis*imidazole, thus obtained, was refluxed with a strong dielectrophile 1,2-*bis*(trifoxy)ethane in acetonitrile solvent, resulting in the formation of macrocyclic tetraimidazolium salts. This tetraimidazolium triflate (**10**) could be reacted with an iron precursor to obtain the Fe(II)-NHC complex, which could be further oxidized with appropriate oxidants to synthesize the high-valent Fe(IV)-oxo complex.

By using the ligands discussed in this section, different research groups [38,41,44,46,48,50,56,59-62] have synthesized a variety of high valent oxidation states in the transition

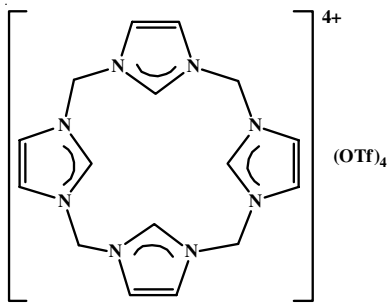

Fig. 5. $[(LNHC)H_4](OTf)_4$, 3,9,14,20-tetraaza1,6,12,17-tetraazoniapentacyclohexacosane-1(23),4,6(26),10,12(25),15,17(24),21-octaene *tetrakis*-trifluoromethanesulfonate (**10**)

metal complexes, as well as utilized these biomimetic complexes in different catalytic reactions. Hence, in the following section, the synthesis of the iron complexes, including the formation and stabilization of their high-valent species will be discussed.

Synthesis of Fe(IV)oxo complexes and their UV-Vis, IR and NMR studies: To understand the structure of reactive intermediates and plausible mechanism of the mononuclear heme/non-heme biological enzymes, bioinorganic chemists have synthesized and characterized many model complexes involving iron. The O-O bond formation or bond cleavage mechanism involving high valent Fe-oxo intermediate is still uncertain in many cases. Synthesis of these Fe-oxo complexes is a challenge to the scientific community because of its limited stability. Herein, the synthetic strategies and stability of the X-ray structurally characterized Fe(IV)oxo complexes, isolated so far, will be discussed. A common protocol was usually followed: the first step is to synthesize the Fe(II)/Fe(III) complexes with the ligand of interest, followed by its oxidation by utilizing various oxidants (peroxides, peroxyacid, ArIO) including molecular oxygen (**Scheme-I**). It has been observed that for majority of the cases, Fe(II)(L) compounds have been characterized by X-ray crystallography. Following the same categorization of ligands, the synthesis and preliminary characterization of the iron complexes is briefly reviewed in Table-1.

In 2003, Que *et al.* [38] reported the spectroscopic properties and the first high resolution crystal structure of a mononuclear non-heme terminal Fe(IV)oxo complex with

Nonheme Ligands (L) (1-10) → **Fe(II)/Fe(III) precursor** → **(L) Fe(II) complex (1A-10A)** → **Oxidant, Low temp.** → **(L) Fe(IV)oxo (1B-*anti*, 1C-*syn*, 1C-*anti*, 1D-*anti*, 2B.OTf, 2B.PF_6, 3B-10B**

Scheme-I: Common protocol for the synthesis of high-valent Fe(IV)oxo complexes

TABLE-1
REACTION CONDITIONS FOR THE SYNTHESIS OF X-RAY STRUCTURALLY CHARACTERIZED Fe(IV)oxo COMPOUNDS AND THEIR STABILITY

Ligand	Fe(II)/Fe(III) precursor	Oxidant	Reaction condition (% yield)	Growth of single crystal	Fe(IV)oxo complex	Axial ligand anti to Fe(IV)oxo unit	Stability	Ref.
1 (TMC)	$[Fe^{II}(TMC)(OTf)_2]$ (**1A.OTf**)	$PhIO/.H_2O_2$	1 eq. PhIO or 3 eq.H_2O_2[a] CH_3CN at –40 °C (90%)	Diffusion of ether in CH_3CN solution at –40 °C	$[Fe^{IV}(O)(TMC)(NCCH_3)](OTf)_2$ **1B-*anti***	CH_3CN	at least 1 month at –40 °C in CH_3CN	[38]
1 (TMC)	$Fe^{II}(TMC)(OTf)_2$ (**1A.OTf**)	2-^{t}BuSO$_2$–C_6H_4IO (ArIO)	Inert N_2 atmosphere, 1 eq. ArIO in anhyd. CF_3CH_2OH, 25 °C	CH_2Cl_2 at –80 °C	$[Fe^{IV}(O_{syn})(TMC)(OTf)](OTf)$ **1C-*syn***	Otf		[59]
1 (TMC)	$Fe^{II}(TMC)(OTf)_2$ (**1A.OTf**)	O_3, Ozone	a) Inert atmosphere, O_3 was bubbled, –80 °C	Green block shaped crystals obtained from reaction mixture	$[Fe^{IV}(TMC)(O_{anti})(OTf)](OTf)$ **1C-*anti***	Otf		[60]
			b) Addition of few micro lit. of H_2O (in CH_2Cl_2), –80 °C to cold solution of **1C-*anti***	Within 2-3 weeks blue crystals were obtained from reaction mixture	$[(H_2O)Fe^{IV}(O)(TMC)](OTf)_2$ **1D-*anti***	H_2O		
2 (TMC-py)	$[Fe^{II}(TMC\text{-}py)](X)_2$, [X= OTf/$PF_6$] **2A.OTf** and **2A.$PF_6$**	1. PhIO	PhIO in CH_3CN/MeOH, RT, (95 %) (followed by crystallization)	CH_3OH layered with Et_2O at -20 °C	$Fe^{IV}(O)(TMC\text{-}py)](X)_2$ [X = OTf or PF_6] **2B.OTf** and **2B.PF_6**	N from dangling Py arm of **2**	7 h at 25 °C ($t_{1/2}$)	[40]
		2. H_2O_2	3 equiv. of H_2O_2 (65 %)				100 min at 25 °C ($t_{1/2}$, in solution)	
		3. $BPh_4^-/HClO_4$	**2A**:BPh_4^-:$HClO_4$ = 1:1:1 (56%)					
		4. O_2/ascorbic acid PhIO	O_2 and ascorbic acid (55%) Excess PhIO in CH_3CN/C_3H_7CN	Layering CH_3CN solution of **3B** with Et_2O at -35 °C	$[Fe^{IV}(O)(TMC\text{-}dma)](OTf)_2$ (**3B**)	Amide O-atom from **3**	» 5 days at 25 °C($t_{1/2}$ in CH_3CN)	[61]
3 (TMC-dma)	$[Fe^{II}(TMC\text{-}dma)](OTf)_2$ (**3A**)							
4 N_4Py	$[Fe^{II}(N_4Py)(CH_3CN)](ClO_4)_2$(**4A**)	Peracetic acid (CH_3CO_3H)/PhIO	6 eq., CH_3CO_3H/2 eq.PhIO taken in CH_3CN at RT	Layering of CH_3CN solution of **4B** with C_5H_{12} at 25 °C	$[Fe^{IV}(O)(N4Py)](ClO_4)_2$ **4B**	Apical N from **4**	60 h at 25 °C	[41]
5 $N_4Py^{2PhF}{}_2$	$[Fe^{II}(N4Py^{2PhF}{}_2)(CH_3CN)](BF_4)_2$ (**5A**)	Isopropyl 2-iodoxybenzoate (IBX-ester)	1.5 eq. IBX-ester at –20 °C	CH_3CN solution of **5B** was layered with Et_2O to obtain yellow crystals at –70 °C	$Fe^{IV}(O)(N4Py^{2PhF}{}_2)](BF_4)_2$ complex (**5B**)	Apical N from **5**		[48]
6, N_2Py_2B B=benzimidazole	$[Fe^{II}(N2Py2B)(CH_3CN)](ClO_4)_2$ (**6A**)	Ceric Ammonium Nitrate, (CAN), $[(NH_4)_2[Ce(NO_3)_6]$	Mixture of 4 equivalents of CAN and $NaClO_4$ in H_2O added to **6A/7A** **6B (62%), 7B (55%)**	Slow evaporation of CH_3CN solution of **6B/7B** mixed with an aq. solution of $NaClO_4$ at 2-5 °C	$[Fe^{IV}(O)(N2Py2B)](ClO_4)_2$ and $[Fe^{IV}(O)(N2Py2Q)](ClO_4)$ **6B and 7B**	Apical N from **6/7**	$t_{1/2}$» 2.5 h, at 25 °C	[50]
7, N_2Py_2Q Q = quinoline	[FeII(N2Py2Q)(OTf)](OTf) (**7A**)							
8 $TMG_3tren\text{-}d_{36}$	$[Fe^{II}(TMG_3tren\text{-}d_{36})(OTf)](OTf)$ (**8A**)	2-^{t}BuSO$_2$-C_6H_4IO	CH_3CN solution of **8A**, reacted with 1 eq of oxidant dissolved in CH_2Cl_2	CH_2Cl_2 solution of perdeuteromethyl complex layered by pentane at -80 °C	$[Fe^{IV}(O)(TMG_3tren\text{-}d_{36})](OTf)_2$ **8B**	Apical N from **8**	30 s at 25 °C	[44]
9	$[Fe^{III}H_3buea(OH)]^-$ and $[Fe^{III}H_3buea(O)]^{2-}$	Ferrocenium tetrafluoroborate ([Fc]BF_4)	**9A** reacted with oxidant in CH_3CN	Crystal obtained after few months from DMF/Et_2O solution at -35 °C in absence of light	$K[Fe^{IV}H_3buea(O)]$ (**9B**)	Apical N from **9**	2.2 h at RT	[62]
10	$[(L^{NHC})Fe^{II}(CH_3CN)_2](OTf)_2$ (**10A**)	2-^{t}BuSO$_2$-C_6H_4IO	**10A** reacted with 3eq. of oxidant in CH_3CN and Et_2O was added at - 40 °C to get $[(L^{NHC})Fe^{IV}O(CH_3CN)](OTf)_2$	Slow diffusion of Et_2O into a solution of $[(L^{NHC})Fe^{IV}O(CH_3CN)](OTf)_2$ in propionitrile (C_3H_7CN)at -40 °C	$[(L^{NHC})Fe^{IV}O(C_3H_7CN)](OTf)_2$ **10B**	C_3H_7CN	5 h at RT	[56]

TMC ligand. Starting from $Fe(OTf)_2.2CH_3CN$ and the TMC ligand, [Fe(II)(TMC)$(OTf)_2$] (**1A.OTf**) complex was synthesized in an inert atmosphere. Oxidation of this complex by using one equivalent of iodosylbenzene (PhIO) or three equivalents of H_2O_2 produced a pale green Fe(IV)oxo intermediate, *trans*-$[Fe^{IV}(O)(TMC)(NCCH_3)](OTf)_2$,(**1B-*anti***) (Fig. 6A) in CH_3CN at –40 ºC with nearly 90% yield. Interestingly, when PhIO was used as an oxidizing agent, the formation of Fe(IV)oxo species was very fast (within 2 min), but when H_2O_2 was used, it took nearly 3 h for the formation. The pale green species showed a absorption maximum at wavelength (λ_{max}) 820 nm (ε, 400 M^{-1} cm^{-1}). Diffusion of ether into the CH_3CN solution of the Fe(IV)oxo species, produced from H_2O_2 oxidation, resulted in blue rectangular parallelopiped crystals, suitable for X-ray crystallography. The high valent oxo species, which was stable for months, in CH_3CN at –40 ºC, started decaying if warmed or was in presence of PPh_3. IR stretching frequency, characteristic of Fe(IV)oxo bond, is observed at 834 cm^{-1} and this band shifts 34 cm^{-1} downward due to isotope labeling (^{18}O).

Subsequently, in 2015, Prakash *et al.* [59] reported another Fe(IV)oxo complex with TMC, $[Fe^{IV}O_{syn})(TMC)(OTf)]$-(OTf) (**1C-*syn***) (Fig. 6B), which was spectroscopically and structurally different (flipped cyclam ring) than the previously reported complex, $[Fe^{IV}O_{anti})(TMC)(NCMe)]^{2+}$ (**1B-*anti***). Interestingly, Que *et al.* [38] speculated that this structural change occurred due to the change in oxidizing agent from PhIO to 2-^{t}BuSO$_2$–C_6H_4IO (ArIO). Bulkier reagents, like ArIO, face restriction in its approach through the *anti*-face. It may be noted that the synthetic strategy followed in this article was different from the previously reported procedures. One equivalent of PhIO or ArIO, dissolved in anhydrous trifluoroethanol was added to CH_3CN/CD_3CN solution of $Fe^{II}(TMC)(OTf)_2$ (**1A.OTf**)

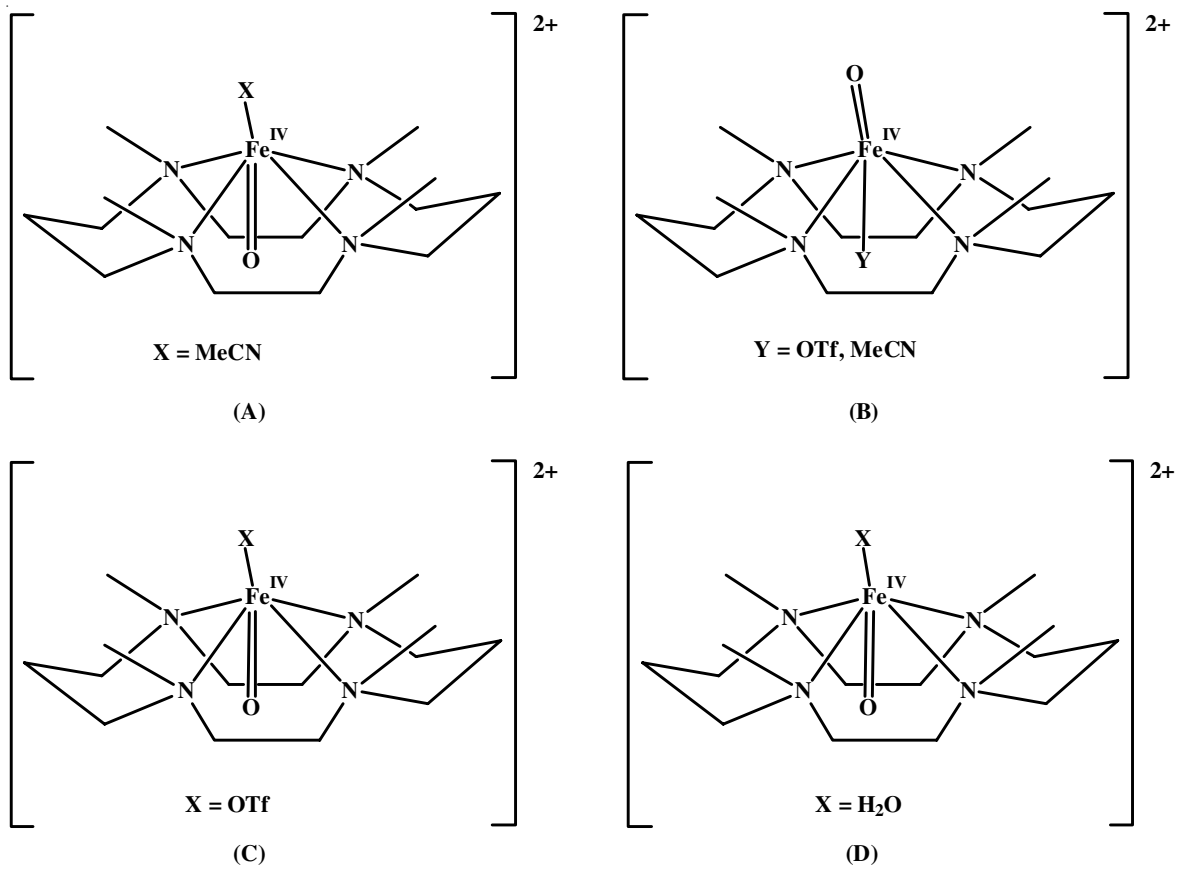

Fig. 6. (A) $[Fe^{IV}(O)(TMC)(NCCH_3)](OTf)2$ (**1B-*anti***), (B) $[Fe^{IV}(O_{syn})(TMC)(OTf)](OTf)$**,** (**1C-*syn***) (C) $[Fe^{IV}$ $(TMC)(O_{anti})(OTf)](OTf)$, (**1C-*anti***), (D) $[(H_2O)Fe^{IV}$ $(O)(TMC)](OTf)_2$ $[Fe^{IV}(O_{syn})(TMC)(OTf)](OTf)$, (**1D-*anti***)

under an inert N_2 atmosphere at 25 ºC to yield **1B-*anti*** and **1C-*syn***, respectively in high yields. The complexes have signature absorption band in the near IR region at 824 nm ($\varepsilon_M = 400$) for **1B-*anti*** and 815 nm ($\varepsilon_M = 380$) for **1C-*syn***. The ESI-MS and IR spectrum of these two complexes also corresponded with the fact that **1B-*anti*** and **1C-*syn*** are different compounds. The effect of axial ligand [CH_3CN in **1B-*anti*** and OTf in **1C-*syn***] bound to the Fe(IV) center *trans* to Fe=O bond are reflected in the Fe=O stretching frequencies. Hence, the stretching frequency is less in case of **1C-*syn***, since OTf is a weaker ligand compared to CH_3CN. Crystals of **1C-*syn***, suitable for X-Ray diffraction, were obtained from the reaction of $Fe^{II}(TMC)(OTf)_2$ with stoichiometric amount of ArIO in CH_2Cl_2 at –80 ºC. Prakash *et al.* [59] distinguished the *anti*- and *syn*-Fe(IV)oxo complexes of TMC (**1B-*anti*** and **1C-*syn***) using ^{1}H NMR spectroscopy. The **1B-*anti*** complex had seven distinctive peaks spanning over 200 ppm, which were paramagnetically shifted from those obtained for ligand **1**. The 1:1:2:2:2:2:6 intensity ratio corresponded to the *trans*-I (R,S,R,S) configuration of **1**, as was observed in case of **1B-*anti***. From the ^{1}H NMR spectra of **1B-*syn***, it was evident that a minor amount of *anti*-Fe(IV)oxo species was present with the majority of the *anti*-compound **1B-*syn*** in the solution. Hence, the peaks observed for **1B-*anti*** were present and distin-guishable from the major peaks of **1B-*syn***, which were again consistent with the 1:1:2:2:2:2:6 intensity ratio, corresponding to the *trans*-I (*R*,*S*,*R*,*S*) configuration of **1**. Contrastingly, the diastereotopic β-CH_2 protons of **1B-*syn*** were sharper and downfield-shifted to 7.3 and 8 ppm, while the N–CH_3 peak was broad and upfield-shifted to –51 ppm, when compared with the peaks of **1C-*syn***.

In 2018, Schaub *et al.* [60] reported an interesting Fe(IV)-oxo compound of TMC ligand using ozone as an oxidant and containing a water molecule as the axial ligand *trans* to the oxo ligand. The use of ozone, as an oxidizing agent for synthesizing Fe(IV)oxo complexes, is not a common practice. Additionally, there were no reports of finding a water molecule as a axial ligand in any high valent oxo-iron non-heme complexes. In 2005, Pestovsky *et al.* [63] first reported a Fe(IV)oxo complex, where ozone was used as an oxidizing agent and in that $[(H_2O)_5Fe{=}O]^{2+}$ species, all the ligands bound with the high spin (S=2) iron center were water, except the oxo ligand. As mentioned earlier, the Fe(II) complex (**1A.OTf**) and Fe(IV)-oxo complex (**1B-*anti***) of TMC was reported by Que *et al*. in 2003 [38]. But the oxidizing agent used were PhIO or H_2O_2. Schaub *et al.* [60] in this report, have synthesized three Fe(II) complexes of TMC, $[Fe^{II}(TMC)(CH_3CN)](OTf)_2$ (**1A.CH_3CN**), $[Fe^{II}(TMC)(OTf)]OTf$ **(1A.OTf)** and $[Fe^{II}(D_{12}$-$TMC)(OTf)]$-OTf (**D_{12}-1A.OTf**) following the synthetic protocol of Rohde *et al*. [38]. Colourless needle shaped crystals of **1A.CH_3CN**, suitable for X-ray analysis were grown by dissolving $[Fe^{II}(TMC)$-$(OTf)]OTf$ (**1A.OTf**) in CH_3CN and letting it slowly evaporate under inert atmosphere. Pink crystals of **1A.OTf** was obtained by chance when a solution of $[Fe^{II}$ $(TMC)(OTf)]OTf$ in CH_2Cl_2 was left in freezer for 4 years. To synthesize this compound

methodically, they used D_{12}-tmc as the ligand, instead of TMC and obtained single crystals of **D_{12}-1A.OTf** within weeks. When ozone was bubbled through the cold (-80 ºC) solution of **1A.OTf** in inert atmosphere, they could successfully synthesize the compound $[Fe^{IV}(TMC)(O_{anti})(OTf)](OTf)$ (**1C-*anti***) (Fig. 6C) as green block shaped crystals, suitable for X-ray crystallography, within a day. When few microliters of water dissolved in CH_2Cl_2 was injected in a cold solution of **1C-*anti*** stored at -80 ºC within 2 to 3 weeks, blue crystals were obtained. On structural analysis, the compound obtained was $[(H_2O)Fe^{IV}(O)(TMC)](OTf)_2$ (**1D-*anti*)** (Fig. 6D) where a water molecule was bound to the Fe(IV) center.

It is worth to observe that the Fe-O unit is destabilized when an anionic ligand (*e.g.* OTf) (**1C-*anti***) is bound at the *trans* position of Fe-O bond. In contrast, CH_3CN stabilizes the Fe(IV)oxo unit most (**1B-*anti***, life-time of 10 h at room temperature). In case of TMC bound Fe-O units, when Fe-O distances obtained from EXAFS data were compared for a series of complexes with various *trans* ligands. It was observed that the anionic ligands like $CN^-/OTf^-/NCS^-/NCO^-/N_3^-/OH^-$ destabilizes the Fe-O units [64]. Triflate anion, in **1C-*syn***, was also found to be loosely bound and spectroscopic evidence showed that when dissolved in CH_3CN, it was easily replaced by the solvent molecule and produced **1B-*syn***.

In this context, Chin *et al.* [65] reported the synthesis of Fe(IV)oxo system using the ligand TmTP (dianion of *meso*-tetra-*m*-tolylporphyrin) and TPP (dianion of tetraphenylporphyrin). There, they exhibited spectroscopically that addition of nitrogen bases, for example, *N*-methylimidazole (for TmTP), pyridine or piperidine (for TPP), to peroxo-bridged Fe(III) porphyrins at -80 ºC in toluene resulted in the formation of Fe(IV)oxo species [65]. Additionally, Nam *et al*. [66] reported the formation of a Fe(IV)oxo complex starting from the Fe(II) precursor of TMC and O_2 in presence of alcohol or ether. Here, the Fe(II) compound was air stable in absence of these solvents. These observations led Thibon *et al.* [40] to modify the tetra-coordinated TMC to penta-coordinated TMC-py, where one of the TMC methyl groups is replaced by 2-pyridylmethyl arm, with the speculation that it will be a better choice for stabilizing Fe(IV)oxo intermediates. Reaction of $Fe(OTf)_2(CH_3CN)_2$ with TMC-py in THF resulted in the formation of Fe(II) complex $[Fe^{II}(TMC\text{-}py)](OTf)_2$ (**2A·OTf**) after appropriate work up. $[Fe^{II}(TMC\text{-}py)](PF_6)_2$ (**2A·PF_6**) was obtained when TMC-py was reacted with $FeCl_2{\cdot}2H_2O$ in MeOH and then $NaPF_6$ was added. Single crystal of $[Fe^{II}(TMC\text{-}py)](PF_6)_2$, suitable for the structural studies, was grown from CH_3CN/MeOH. High valent Fe(IV)oxo complex of TMC-py was obtained using two different pathways, one was using a traditional pathway of utilizing an oxidant or oxygen atom donor like PhIO or H_2O_2 and another way was utilized a reductant and a proton donor, *e.g.* BPh_4^-/H^+ or ascorbic acid. When $[Fe^{II}(TMC\text{-}py)]X_2$ (X = OTf or PF_6) *i.e.* **2A·OTf** and **2A·PF_6** was reacted with excess of PhIO in acetonitrile/methanol, a pale brown green complex $[Fe^{IV}(O)(TMC\text{-}py)](X)_2$ (X = OTf or PF_6) [**2B·OTf** and **2B·PF_6**] with 95% yield was obtained at room temperature (Fig. 7A). Electronic spectrum of this compound shows a ligand-field band at 834 nm (ε_{max} = 260 M^{-1} cm^{-1}). Highly stable crystals suitable for X-ray crystallography were obtained from MeOH layered with Et_2O at -20 ºC ($t_{1/2}$ = 7 h at 25 ºC). Same Fe(IV)oxo complex could be generated when Fe(II) precursor was reacted with three equivalents of H_2O_2 but with a lower yield of 65 %. The higher stability of this newly synthesized Fe(IV)oxo complex of TMC-py, compared to the complex synthesized from TMC, can be attributed to the influence of the different coordinative properties due to presence of 2-pyridylmethyl arm in the pentadentate ligand. Consequently, in FTIR, Fe(IV)oxo stretching frequency was observed at 13 cm^{-1} lower value than the corresponding TMC complex.

In this report, dioxygen activation study of Fe(II) complex was also discussed in presence of a reductant *e.g.* BPh_4^- and acid (namely, $HClO_4$) or ascorbic acid. When an oxygenated solution of **2A** was treated with BPh_4^- and $HClO_4$ acid in the ratio **2A**:BPh_4^-:$HClO_4$ = 1:1:1, complex **2B** ($t_{1/2}$ = 100 min) with a lower stability and 56 % yield was obtained. In an oxygenated solution of **2A** in 1:1 mixture of CH_3CN and EtOH, when ascorbic acid (0.5 equivalents) was added, it afforded **2B** in about 55% yield. A reductive activation mechanism is proposed for the conversion of **2A** to **2B** *via* a Fe(III)OOH intermediate and subsequent cleavage of O-O bond by homolytic or heterolytic fashion (*via* probably a short lived Fe(V) species) [40].

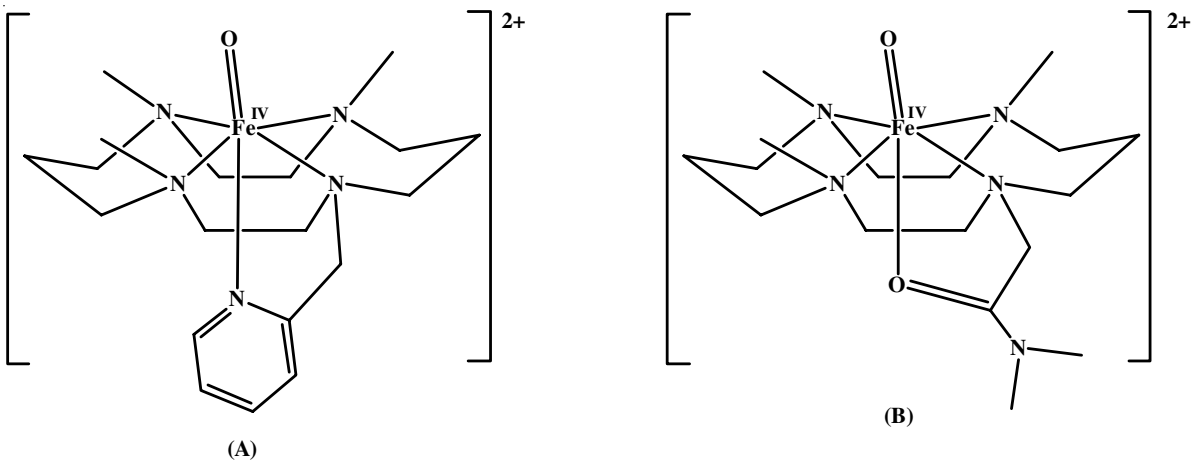

Fig. 7. (A) $Fe^{IV}(O)(TMC\text{-}py)](X)_2$, [X = OTf or PF_6], (**2B**.OTf) (B) $[Fe^{IV}(O)(TMC\text{-}dma)](OTf)_2$, (**2B**.$PF_6$)

Until 2014, when the highly stable Fe(IV)oxo complex of cyclam ligand TMC-dma (**3**) [**3** = 1,4,8-Me_3cyclam-11-CH_2C-(O)NMe_2)] [Fe^{IV}(O)(TMC-dma)]$(OTf)_2$ (**3B**) was crystallographically characterized, compound **2B** (with TMC-py ligand) was considered to be the most stable complex. Compound **3B** had a longer half-life ($t_{1/2}$) of 5 days in acetonitrile at 25 ºC compared to compound **2B** ($t_{1/2}$ = 7 h at 25 ºC) or **4B** ($t_{1/2}$ = 60 h at 25 ºC). The uniqueness of pentadentate ligand **3** lies in the fact that it contains a dimethylacetamido O-atom donor which coordinates to the iron center making the Fe complexes a suitable model complex for many non-heme enzymes found in nature.

The Fe(II) complex of **3** was synthesized by reacting the ligand with Fe $(OTf)_2(CH_3CN)_2$ in THF. After appropriate work up, crystals of [Fe^{II}(TMC-dma)]$(OTf)_2$ (**3A**) suitable for X-ray analysis were grown by vapour diffusion of Et_2O into a conc. CH_3CN solution. Similar to other Fe(II) complexes of TMC group of ligands, this compound also have a *trans*-I configuration of cyclam ligand. Pale brown solution of Fe(IV)oxo complex **3B** was synthesized by reacting **3A** with excess PhIO in acetonitrile/butyronitrile (Fig. 7B) [61]. High stability of this species allowed the growth of single crystals suitable for X ray crystallography by layering CH_3CN solution of **3B** with Et_2O at -35 ºC. Electronic spectrum (λ_{max} = 810 nm, ε_{max} = 270 M^{-1} cm^{-1}) and IR band of this complex has a typical value corresponding to S=1, Fe(IV)oxo complexes reported so far. Furthermore, England *et al.* [44] found that when **3B** was reacted with a base, tetraalkylammonium hydroxide (NBu_4OH) or methoxide in CH_3CN, it produced a blue coloured solution (λ_{max}= 588 nm and ε = 460 M^{-1} cm^{-1}) of Fe(IV)oxo species (**3B′**) with less stability in room temperature ($t_{1/2}$ ~ 1.5 h at 0 ºC), however, moderately stable at -40 ºC. They proposed the newly generated species as conjugate base of **3B** as [Fe^{IV}(O)(L-H)](OTf) (**3B′**).

Belonging to the second category of non-heme ligands, a variety of high valent Fe(IV)oxo complexes were subsequently synthesized by different research groups. A reaction of almost equimolar amounts of N4Py ligand and $Fe(ClO_4)_3 \cdot 10H_2O$ in a mixed solvent of methanol and acetonitrile, produced the Fe(II) complex, $[Fe(N4Py)(CH_3CN)]^{2+}$ (**4A**) as dark red crystalline solid. When this Fe(II) complex was further reacted with six equivalents of peracetic acid, CH_3CO_3H, at room temperature, it produced the green $[Fe^{IV}(O)(N4Py)]^{2+}$ species (**4B**) (Fig. 8A) [43]. The **4B**, with half-life of 60 h, could also be obtained by oxidizing the Fe(II) complex with two equivalents of PhIO. The final product was crystallized by layering C_5H_{12} over a solution of Fe(IV)oxo complex in acetonitrile [41]. Interestingly, the green species exhibited a band at 695 nm (ε = 400

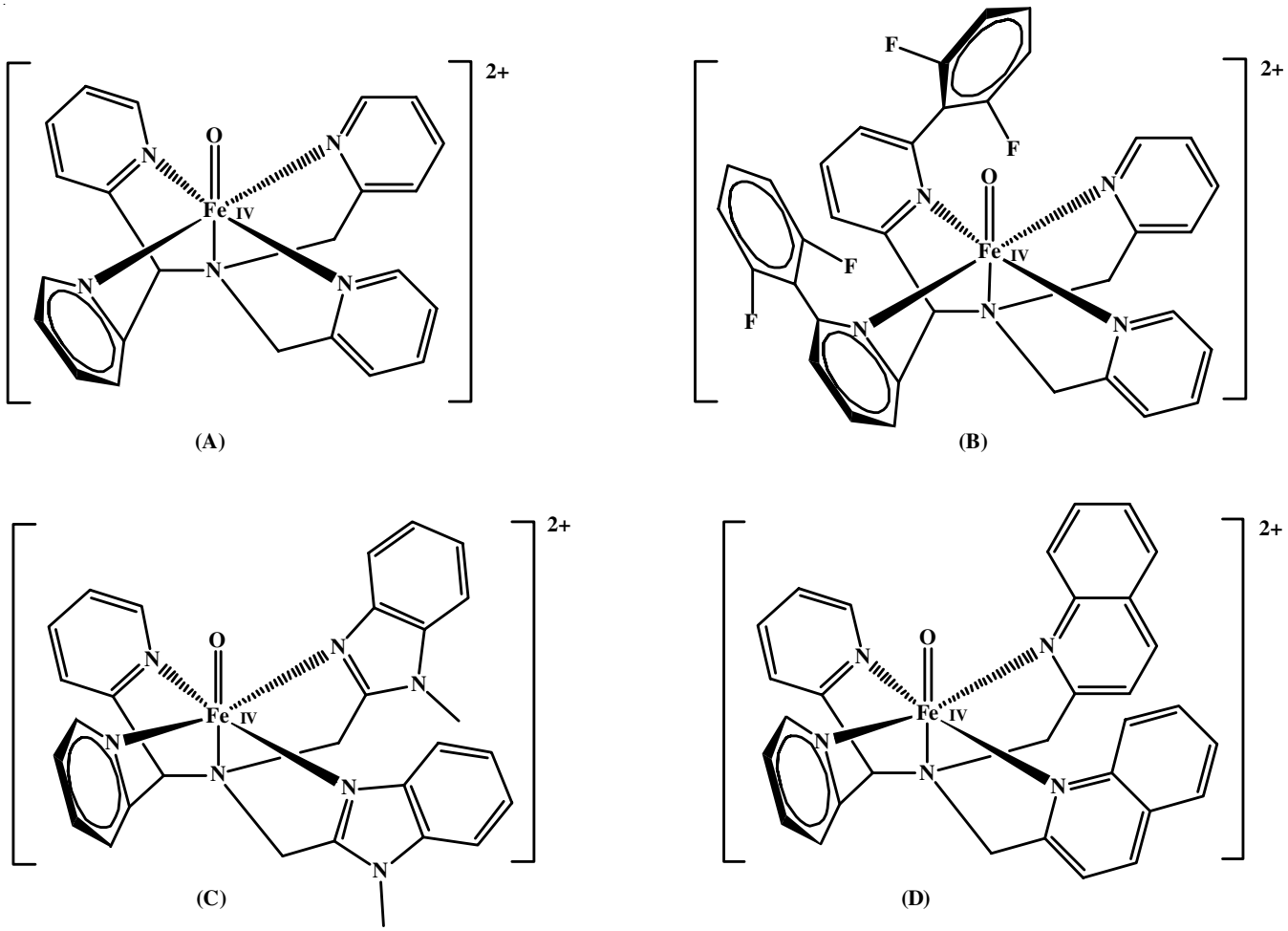

Fig. 8. (A) [Fe^{IV}(O)(N4Py)] $(ClO_4)_2$, (B) Fe^{IV}(O)($N4Py^{2PhF_2}$)]$(BF_4)_2$, (**4B**) (C) [Fe^{IV}(O)(N2Py2B)]$(ClO_4)_2$, (**5B**) (D) [Fe^{IV}(O)(N2Py2Q)](ClO_4), (**6B**) [B=benzimidazole, Q = quinoline]

$M^{-1C\text{-}syn}m^{-1}$) in acetonitrile, while the Fe(II) species, in acetone, could be observed at 458 nm (ε = 4000 $M^{-1C\text{-}syn}m^{-1}$). The ^1H NMR was also helpful in identifying the Fe(IV)oxo species, since the low spin S = 1 complex enabled well-resolved sharp peaks for the protons in the molecule, spanning upto 200 ppm. The highly symmetric nature of the $[Fe^{IV}(O)(N4Py)]^{2+}$ species led to the presence of two sets of protons on the different pyridine rings, one of which was shifted upfield, while the other was shifted downfield.

In 2016, Goldberg *et al*. [48] reported the synthesis and catalysis of three Fe(IV)oxo complexes. Previously, in 2014, they reacted the $N4Py_2^{2PhF}$ with equivalent amounts of $Fe(BF_4)_2 \cdot 6H_2O$ in acetonitrile, to obtain $[Fe^{II}(N4Py_2^{2PhF})(CH_3CN)](BF_4)_2$ (**5A**) as dark red crystals [47], which was further reacted with isopropyl ester of iodoxy benzoic acid (1.5 equiv.) at -20 ºC to obtain the desired $[Fe^{IV}(O)(N4Py_2^{2PhF})](BF_4)_2$ complex (**5B**) (Fig. 8B), which was stable at the same temperature for ~ 4 h. In order to get high resolution X-ray crystals, an acetonitrile solution of **5B** was layered with diethyl ether to obtain yellow crystals at –70 ºC [48]. While the Fe(II) complex **5A** showed two distinct peaks at 370 nm and 460 nm, these were replaced by a weak band at 750 nm (ε = 250 M^{-1} cm^{-1}) for the Fe(IV)oxo **5B** complex. But, when the temperature was increased to 23 ºC, an intense band appeared at 785 nm, due to the generation of a Fe(III) species through intramolecular hydroxylation of the aromatic ring.

Continuing the search for thermally stable and catalytically active Fe(IV)oxo complexes, Que *et al*. [50] reported two structurally characterized molecules with the pentadentate N2Py2X ligand framework (X = quinoline (Q) and benzimidazole (B). The Fe(II) complexes with **6** and **7** were obtained from the reaction between the respective ligands and $Fe^{II}(OTf)_2 \cdot 2CH_3CN$. Under anaerobic conditions, the Fe(II) complex, $[Fe^{II}(N2Py2B)(CH_3CN)](ClO_4)_2$ (**6A**) was synthesized as a red solid, which was further reacted with a mixture of four equivalents of ceric ammonium nitrate and sodium perchlorate in H_2O, to obtain the Fe(IV)oxo complex of N2Py2B, $[Fe^{IV}(O)(N2Py2B)](ClO_4)_2$ (**6B**) as a greenish-blue powder (Fig. 8C). A solution of **6B** was mixed with an aqueous solution of $NaClO_4$ and allowed to evaporate slowly at 2-5 ºC, which afforded bluish green high resolution X-ray crystals. Following the same procedure for N2Py2Q, in nitrogen atmosphere, Fe(II) complex $[Fe^{II}(N2Py2Q)OTf]OTf$ (**7A**) was obtained as a dirty yellow solid. Subsequently, reaction with CAN and $NaClO_4$ produced a dark green Fe(IV)oxo complex, $[Fe^{IV}(O)(N2Py2Q)](ClO_4)_2$ (**7B**) (Fig. 8D), which was crystallized by following the same procedure as **6B**.

In 2010, two different research groups, Que [44] and Borovik [62], reported the successful structural characterization of crystalline Fe(IV)oxo complexes with tripodal N4 ligands. England *et al*. [44] reported the reaction of $TMG_3tren\text{-}d_{36}$ (**8**) with $Fe^{II}(OTf)_2(CH_3CN)_2$ to synthesize $[Fe^{II}(TMG_3tren\text{-}d_{36})(OTf)](OTf)$ (**8A**) as white powder. The subsequent oxidation of **8A** with equivalent amount of 2-(*tert*-butylsulfonyl)iodosylbenzene (2-^{t}BuSO$_2$C$_6$H$_4$IO), provided the orange coloured Fe(IV)oxo complex $[Fe^{IV}(O)(TMG_3tren\text{-}d_{36})](OTf)_2$ (**8B**) (Fig. 9A).

Borovik *et al*. [62] utilized *tris*[(N-*tert*-butylureaylato)-N-ethyl)]aminato ligand (**9**) and ferrous acetate, in presence of strong base, KH to obtain $K[Fe^{III}H_3buea(OH)]$ (**9A**) as dark red crystals. To obtain the desired Fe(IV)oxo product, $K[Fe^{IV}H_3buea(O)]$ (**9B**) (Fig. 9B), the Fe(III) complex was dissolved in acetonitrile and oxidized by ferrocenium tetrafluoroborate ($[Fc]BF_4$) and a brown precipitate was obtained from that reaction in 35% yield at room temperature. The **9B** was recrystallized from a DMF/ether solution at -35 ºC in absence of light. While **9A** could be recognized by the strong absorption band at 400 nm (ε_M = 5000 nm), the presence of 808 nm (ε_M = 280 nm) proved the formation of Fe(IV)oxo (**9B**) species. A solution of **9B** in DMF had a half-life of 2.2 h at room temperature, after which it reverted back to **9A**, the C-H bond activation of the solvent molecule.

Meyer *et al*. [56] reacted the macrocyclic tetraimidazolium triflate (**10**) with $[Fe\{N(SiMe_3)_2\}_2]_2$ in acetonitrile to produce the Fe(II) complex $[(L^{NHC})Fe^{II}(CH_3CN)_2](OTf)_2$ (**10A**) in ~30% yield, which was further oxidized by 2-^{t}BuSO$_2$C$_6$H$_4$IO to obtain green Fe(IV)oxo complex $[(L^{NHC})Fe^{IV}O(CH_3CN)](OTf)_2$ at -40 ºC. Single crystals of $[(L^{NHC})Fe^{IV}O(C_3H_7CN)](OTf)_2$ (**10B**) (Fig. 10) were obtained from the slow diffusion of diethyl ether into a solution of $[(L^{NHC})Fe^{IV}O(CH_3CN)](OTf)_2$ in propionitrile (C_3H_7CN) at -40 ºC. Interestingly, the oxidation with diatomic oxygen was also carried out, but the dinuclear Fe(III) complex was obtained having a bridging O-atom. It is also observed that **10B** was also converted to the same Fe(III) complex, when the temperature of the solution was gradually increased from -40 ºC.

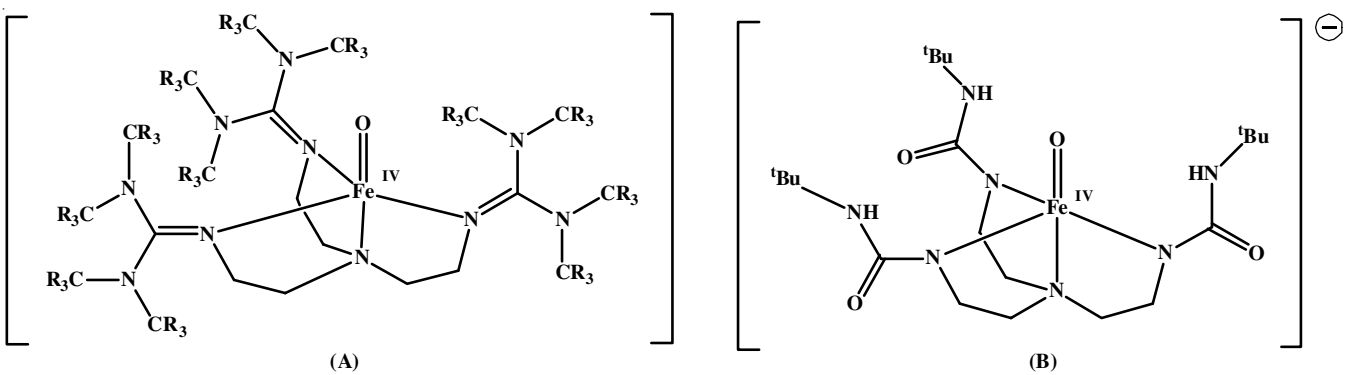

Fig. 9. (A) $[Fe^{IV}(O)(TMG_3tren\text{-}d_{36})](OTf)_2$, (**8B**) (B) $K[Fe^{IV}H_3buea(O)]$, (**9B**)

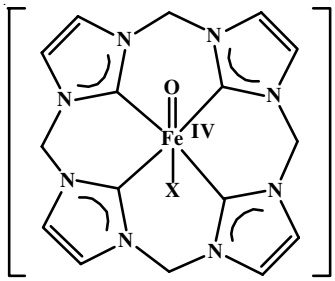

Fig. 10. $[(L^{NHC})Fe^{IV}O(C_3H_7CN)](OTf)_2$, (**10B**)

Crystallographic characterization of Fe(IV)oxo complexes: Herein a detailed discussion about the crystallographic parameters for the X-ray structurally characterized non-heme oxoiron(IV) complexes were carried out. According to the previous categories, these Fe(IV)oxo complexes have been divided into three major groups, namely, TMC-cyclam type ligands, N4Py frameworks and tripodal N4 ligands. The crystallographic parameters, *e.g.* Fe-O distance, Fe-N_{av} distance, Fe-L_{axial} (N/O) distance, angle between mean equatorial plane of L & Fe=O (°), *trans*-L_{axial}(N/O)- Fe=O angle (°) *d*-values for the above mentioned complexes are tabulated in Table-1.

Catalytic activity mimic of biological molecules: Macrocyclic TMC ligand is one of the important class of ligands for bio-mimicking the high valent Fe(IV)oxo intermediate present in the catalytic cycle of various non-heme proteins or enzymes. Some of the important crystallographic data of six high-valent (**1B-*anti***, **1C-*syn***, **1C-*anti***, **1D-*anti*, 2B & 2C**) non-heme mononuclear Fe(IV)oxo complexes comprising of TMC ligand, where Fe center is in an octahedral environment, will be discussed and compared. In equatorial plane, Fe is bound with four nitrogen atoms from the cyclam ligand and one of the axial position is occupied by dianionic oxo ligand. The main difference between complexes **1B**, **1C** and **1D** lies in the nature of axially coordinated ligand present *trans*- to the oxo group. This position is occupied either by solvent molecule like CH_3CN (**1B-*anti***) or by monoanionic triflate (OTf) (**1C-*syn*** & **1C-*anti***) or by water molecule (**1D-*anti***) [60] added externally. In other two structurally Fe(IV)oxo complexes (**2B** and **3B**), modified TMC ligands were used with pendant (tethered) arms. Compound **2B** contains 2-pyridylmethyl arm (N donor) while compound **3B** has *N,N*-dimethylacetamide arm (O donor), which was appended to the cyclam framework. Que *et al*. [38] were first to report the structurally characterized Fe(IV)oxo compound **1B-*anti*** in a nonporphyrin ligand environment in the year 2003. In 2015, Que *et al*. [59] further synthesized, two Fe(IV)oxo complexes **1B-*syn*** and **1C-*syn***, where "oxo" ligand occupies the "*syn*" face of the ligand by changing the oxidizing agent from PhIO to ArIO (2-^{t}BuSO$_2$-C$_6$H$_4$IO). They proposed that the s*yn*-isomer is formed due to the steric hindrance caused by ArIO, which does not allow the attack of oxidant at the *anti*-face of Fe(II) precursor. In both complexes, the structural flip was evidenced by spectroscopic data, which were similar but with distinct features from previously synthe-sized **1B-*anti*** complex. Additionally, crystallographic data for **1C-*syn*** strongly supported the proposed "*syn*" structure of the compound, where instead of CH_3CN, triflate was bound as the axial ligand *trans* to the oxo group. Subsequently, in 2018, Schindler's research group [60] successfully reported a structurally characterized Fe(IV)oxo compound (**1C**), where oxo ligand is present in the "*anti*" face of the TMC ligand. The main difference in synthetic protocol was the use of a different oxidant, ozone. So, from these observations, it can be safely concluded that oxidizing agents have a key role in deciding *syn* or *anti* structure of these Fe(IV)oxo compounds. When water was injected in a cold solution of **1C-*anti***, it produced **1D-*anti*** by replacing the axially bound OTf anion. No structural flip was observed due to change in the axial ligand *trans* to the oxo group. Further information obtained from the crystals, showed that the asymmetric unit of light blue coloured triclinic crystals of **1B-*anti*** contains a cationic iron complex and have two triflate counter anions, with $P\bar{1}$ space group. Triflate anions are either disordered or have thermal motions. The monoclinic blue-green crystals of **1C-*syn*** with space group $P2(1)/n$ was the first example of Fe(IV)oxo compound where TMC was found in a *syn*-structure. X-ray data revealed that the green coloured crystals of "*anti*" version of **1C** had an orthorhombic space group $P2_12_12$. Crystal structure of **1C-*anti*** was refined as 4-component twin and both components were found to be racemically twinned also. The asymmetric unit had four TMC and triflate bound Fe(IV)oxo units along with four non-coordinated triflate anions and four CH_2Cl_2 as solvents of crystallization. Crystallographic analysis of the other unusual H_2O bound complex **1D-*anti*** was found to have orthorhombic crystals with $C222_1$ space group and it was racemically twined. There were half molecule of Fe(IV)oxo unit, one triflate anion and two half dichloromethane molecules present in the asymmetric unit of **1D-*anti***.

Crystallographic studies: The Fe-O distance found in complex **1B-*anti*** is 1.646(3) Å and matches with many Fe(IV)-O distances found in synthetic porphyrin complexes (1.62 to 1.67 Å) [67,68]. In **1C-*syn***, the Fe-O distance is 1.625(4) Å, which is 0.02 Å shorter than that found in **1B-*anti*** [1.646(3) Å] and 0.042 Å shorter than that found in **1C-*anti*** [1.667(9) Å]. In *anti* compounds where neutral ligands like CH_3CN (**1B-*anti***) or H_2O (**1D-*anti***) were the *trans* ligands, the Fe-O bond distances are in comparable range: $r_{Fe\text{-}O}$ (**1B-*anti***) [X = CH_3CN,1.646(3) Å] ~ $r_{Fe\text{-}O}$ (**1D-*anti***) [X = H_2O, 1.650(2) Å]. Four different sets of Fe-O bond distances, 1.636(8) Å, 1.644(7) Å, 1.652(7) Å,1.667(9) Å were found for four molecules present in one asymmetric unit of **1C-*anti***. This reduced Fe-O bond distance also supports the terminal nature of Fe-O bond where the Fe is in +4 oxidation state and have a double bond character.

Typical Fe-O terminal bond distances found so far in structurally characterized Fe(III)oxo complexes are quite long and falls in the range 1.79 to 1.82 Å [69-71]. In $Fe_2(\mu\text{-}O)_2$ diamond core, $[Fe^{III}_2(\mu\text{-}O)_2(6\text{-}Me_3\text{-}TPA)](ClO_4)_2$ [6-Me_3-TPA = *tris*(6-methylpyridyl-2-methyl)amine], the Fe-μ-O distances are of 1.8 and 1.92 Å [72] while in case of dioxo-bridged $[Fe^{IV}_2(\mu\text{-}O)_2(Lb)_2]^{4+}$ [Lb = *tris*(4-methoxy-3,5-dimethylpyridyl-2-methyl)-amine] [73]. The EXAFS data reveals a Fe(IV)-μ-O distance of 1.77 Å and in $[Fe_2(\mu\text{-}O)_2(5\text{-}Et_3\text{-}TPA)_2](ClO_4)_3$, the $Fe^{III}Fe^{IV}$

Fe-μ-O [74] distance as 1.83 Å. The Fe-O bond distances in Fe^{IV}-O-Fe^{IV} species containing TAML ligand, a tetraamidato macrocyclic, (where TAML = 3,3,6,6,9,9-hexamethyl-3,4,8,9-tetrahydro-1*H*-1,4,8,11-benzotetraazacyclotridecine-2,5,7,10-(6*H*,11*H*)-tetraone)] lies in the range 1.728 to 1.744 Å [75].

Now, the Fe-X (X=O/N) bond lengths present *trans*- to the Fe-oxo bond are compared, it is observed that Fe-N(CH_3CN) bond distance found in the crystal structure of **1B-*anti*** was 2.058(3) Å. The Fe-O(OTf) bond present in **1C-*syn*** was quite longer 0.088 Å compared to **1B-*anti***. Four Fe-O(OTf) bond distances found in one asymmetric unit of **1C-*anti*** were 2.064(8) Å, 2.054(8) Å, 2.054(7) Å and 2.053(7) Å. The Fe-O(H_2O) bond found in **1D-*anti*** [2.049(2) Å] is shorter than Fe-O(OTf) bond present in **1B-*anti*** or **1C-*syn***. The average Fe-N(TMC) bond lengths present in the equatorial plane of the octahedral, *i.e.* Fe-L(eq) value found in the crystal structure of **1B-*anti***, **1D-*anti*** and **1C-*syn*** were 2.09 Å, 2.084 Å and 2.066 Å, respectively. So the Fe-N(TMC) bond present in **1C-*syn*** was quite shorter 0.024 Å compared to **1B-*anti***. The Fe-L_{eq} found in **1C-*anti*** were 2.082 Å, 2.098 Å, 2.078 Å and 2.102 Å. The value is shortest in **1C-*syn*** compound. So, the crystallographic studies revealed that one Fe-O(oxo) and four Fe-N(TMC) bond distances present in **1C-*syn*** were shorter compared to the bonds present in **1B-*anti***. These cumulative shortening of bond-lengths (~ 0.1 Å) were compensated by a longer Fe-O(OTf) bond present *trans* to the Fe-O(oxo) bond in **1C-*syn***. The density functional theory calculations showed that the Fe atom was 0.03 Å and 0.07 Å above the TMC plane in **1B-*anti*** and **1C-*syn***, respectively [76]. These values, further support the trend found in various Fe-Ligand bond lengths. If the average of all the metal-ligand bond distances present in TMC bound Fe(IV)-oxo compounds are considered, the Fe-L(av) distances found in **1B-*anti***, **1D-*anti*** and **1C-*syn*** were 2.084 Å, 2.077 Å and 2.082 Å. In **1C-*anti***, these Fe-L(av) distances were 2.079 Å, 2.089 Å, 2.073 Å and 2.092 Å. Thus, $r_{Fe\text{-}N\ (\mathbf{1D\text{-}anti})}$ [2.077 Å] < $r_{Fe\text{-}N\ (\mathbf{1C\text{-}syn})}$ [2.082 Å] < $r_{Fe\text{-}O\ (\mathbf{1B\text{-}anti})}$ [2.084 Å].

Two more important Fe(IV)oxo compounds were structurally characterized, using modified pentadentate TMC ligands (**2** and **3**) were compound **2B·(OTf)$_2$** and **3B**. Substituted TMC ligands (**2** and **3**) not only imposes more steric bulk to the axial ligand, but also causes geometric constraints to the cyclam ring due to tethering a donor arm substituting a methyl group. Crystal structural analysis of triclinic single crystals of **2B·(OTf)$_2$** with space group $P\bar{1}$ confirmed the coordination of TMC-py ligand as a pentadentate ligand and the cyclam ligand had a *trans*-I stereochemistry. Highly stable ($t_{1/2} \approx 5$ days at 25 ºC), monoclinic crystals of 3B with $P2_{1/n}$ space group was the first X-ray structurally characterized Fe(IV)oxo compound where an O-atom donor was present *trans* to Fe=O bond. Later on three more structurally characterized complexes, *i.e.* **1C-*syn***, **1C-*anti*** and **1D-*anti*** with O-donor *trans* to Fe=O bond were added to the series. When the bond distances found in the TMC/substituted TMC bound Fe(IV)oxo complexes were compared, Fe=O(oxo) bond [1.667(3) Å] present in **2B·(OTf)$_2$** is the longest one compared to **3B** [1.658(1) Å], **1B-*anti*** [1.646 (3) Å] and **1D-*anti*** [1.650(2) Å]. In addition, the Fe-$N_{amine(av)}$ bond distance in **2B·(OTf)$_2$** had a comparable value (2.083 E) with **1B-*anti*** (2.09 Å) or **1D-*anti*** (2.083 Å). Compared to these Fe(IV)oxo complexes reported thus far, the Fe-$N_{amine(av)}$ distance is shorter in **3B** (2.060 Å) and **1C-*syn*** (2.066 Å). But Fe-Npy axial bond distance 2.118(3) Å, is quite longer (0.06 to 0.07 Å) compared to Fe-N(CH_3CN) or Fe-O(H_2O) axial bonds present in **1B-*anti*** (2.058 Å) or **1D-*anti*** (2.049 Å). The Fe-O_{amide} axial bond length in complex **3B** is only 1.981(1) Å and considered to be the shortest among all other structurally characterized Fe(IV)oxo compounds. Greater donor strength of dimethyl-acetamido ligand, due to the contribution from the resonance structure characteristic of amide group, was responsible for this observation [77,78]. Longer Fe-Npy axial bond distance is in contrary with the fact that pyridine is a stronger base than CH_3CN or H_2O. Two factors play important role here, steric bulk of ligand and the N_{py}-O=Fe angle. The N_{py}-O=Fe angle deviates quite a bit from linearity in **2B·(OTf)$_2$** [169.8(2)º] and **3B** [175.6(6)º]. The *trans* O/N-Fe=O angle were nearly linear in **1B-*anti*** 178.9(1)º and perfectly linear 180.0° linear in **1D-*anti***. The *trans* O/N-Fe=O angle increasingly deviates from linearity in the order of **1D-*anti*** [180.02º] < **B-*anti*** [178.9°] < **3B** [175.6º] < **2B.(OTf)$_2$** [169.8º]. This further regulates the Fe-N/O axial bond lengths by controlling the *trans* effect of the oxo ligand present *trans* to it. The Fe-N/O axial bond lengths increases in the order of **3B < 2B-*anti* ≈ 2D-*anti* < 2B·(OTf)$_2$.** Important structural parameters of Fe(IV)oxo complexes of ligands, **1**,**2** and **3** are tabulated in Table-2.

The second reported crystal structure of a Fe(IV)oxo species is that of green monoclinic [Fe^{IV}(O)(N4Py)](ClO_4)$_2$ complex (**4B**), containing two solvent molecules of acetonitrile, with space group *C*m [41]. As expected, it was compared with the first reported **1B-*anti*** complex, wherein it was observed that the Fe=O bond distance of **4B** [1.639(5) Å] was extremely close to that of **1B-*anti*** [1.646(3) Å]. Another comparison showed that the equatorial Fe-N bond lengths [av. 1.957(5) Å] were reduced by 0.1 Å from those of **1B-*anti***, which can be explained by the greater bonding ability of a pyridine moiety than a *tertiary* amine. Other notable feature is the Fe-N1 (*trans* to oxo ligand) bond length of 2.033(8) Å, which is the longest metal-ligand bond in complex **4B**. The oxo-ligand, Fe-atom and bridging N-atom of N4Py ligand are almost collinear, with the angle being 178.6(3)º. In 2016, Goldberg *et al*. [48] had reported a similar crystal structure of Fe(IV)oxo complex, bearing the substituted N4Py ligand. Here, they observed that in [Fe^{IV}(O)($N4Py_2^{2PhF}$)](BF_4)$_2$ complex, the Fe=O was quite short [1.6600(16) Å]. While the average length of Fe-N_{eq} bonds were 2.004 Å, the axial one [2.051(2) Å] was definitely longer than the equatorial ones. Additionally, a slight tilt between the Fe=O and the equatorial plane was observed, the angle being 86.9º between the average plane of the ligand and the Fe=O. Here also, a solvent molecule of acetonitrile was present within unit cell and the distance between the $H_{acetonitrile}$ and O was [2.54(3) Å], indicating the presence of hydrogen bonding interaction. Further, two crystals of Fe(IV)oxo species belonging to the similar class of ligands were reported in 2018 and interestingly [50], the Fe=O were observed to be longer than in **4B**, as in 1.656(4) Å (**6B**) and 1.677(5) Å in (**7B**). This is justified by the fact that two pyridines of **4B** were replaced by

TABLE-2
COMPARISON OF STRUCTURAL DATA FOR **1B-*anti***, **1C-*syn***, **1C-*anti***, **1D-*anti***, **2B** AND **3B** CONTAINING MACROCYCLIC LIGANDS

Ligand	Fe(IV)O	$(Fe–L)_{av}$ (Å)	$(Fe–L_{eq})_{av}$ (Å)	$Fe–L_{ax}$ (Å)	Fe=O (Å)	Angle b/w mean equatorial plane of L & Fe=O (°)	*trans*-O/N–Fe=O angle (°)	Ref
1	**1B-*anti***	2.084	2.090	2.058(3)	1.646(3)	87.5	178.9(1)	[38]
1	**1C-*syn***	2.082	2.066	2.146(2)	1.625(4)	86.9	175.3(7)	[59]
1	**1C-*anti***	2.077	2.084	2.049(2)	1.650(2)	90.0	180.0	[60]
1	**1D-*anti***	2.079	2.082	2.064(8)	1.636(8)	87.9	177.0(3)	[60]
		2.089	2.098	2.054(8)	1.644(7)	85.5	179.6(3)	
		2.073	2.078	2.054(7)	1.652(7)	87.7	177.5(3)	
		2.092	2.102	2.053(7)	1.667(9)	85.1	178.8(4)	
2	**2B**	2.09	2.083	2.117(5)	1.667(4)	87.4	169.8(2)	[40]
3	**3B**	2.044	2.060	1.981(1)	1.658(1)	89.9	175.6(6)	[61]

N-methylbenzimidazoles in **6B** and quinolines in **7B**, thereby altering the steric and electronic environment around the Fe(IV)oxo centers. Concomitantly, an increase in the average bond length of Fe–N was also observed as 1.999 Å in **6B** and 2.053 Å in **7B**. Another steric effect of the bulkier moieties was the increasing tilt of the Fe=O moiety from the *trans*-N atom as in 179.4(3)º (**4B**) to 177.40(8)º (**5B**) to 177.0(2)º (**6B**) to 170.5º (**7B**). There also exists a trend in the $Fe–N_{eq}$ bond lengths due to the increasing basicity of the different heterocyclic species, which leads to greater *trans* effect, for example, 1.957 Å in **4B** to 1.971 Å in **6B** to 2.049 Å in **7B**. It is also observed that **5B** does not follow the trend since the greater steric effect outweighs the electronic factor. Important structural parameters of Fe(IV)oxo complexes of ligands, **4**, **5**, **6** and **7** are tabulated in Table-3.

Among the Fe(IV)oxo complexes of tripodal N4 ligands, it was observed that the Fe=O bond distance was considerably short in **8B** [1.661(2) Å] and **9B** [1.680(1) Å]. In contrast, the average bond lengths of $Fe\text{-}N_{equatorial}$ were longer **8B** [2.005 Å] and **9B** [1.988 Å], when compared with **4B** [1.957 Å], but shorter than **1B-*anti*** [2.091 Å]. Such an observation can be expected due to the highly basic peralkylguanidinyl donors and also due to the decrease in coordination number **8** and **9** ligand frameworks. Interestingly, the dissimilar $Fe\text{-}N_{ax}$ and $Fe\text{-}N_{eq}$ bond lengths can be justified by the high *trans* effect of the oxo-donor. Another interesting feature in these tripodal N4 ligands was the provision for intramolecular hydrogen bonding, which would further stabilize the Fe(IV)oxo moieties. Hence in complex **8B**, since the perdeuterated ligand was utilized, three symmetrical non-bonding interactions were observed between the C-D···O with the distance ranging from 2.38 Å to 2.49 Å. Similarly, in **9B**, a similar set of three N-H···O hydrogen bonding interactions are observed.

N*-Heterocyclic carbenes complexes:** Another different ligand framework based on the *N*-heterocyclic carbenes was reported by Meyer *et al*. [56] to synthesize a Fe(IV)oxo species, which produced green crystals. The orthorhombic space group P_{bca} was found in **10B**, where coordination of the four carbenes species to the Fe(IV) afforded a planar structure, with the oxo ligand placed *trans* to a solvent molecule. Interestingly, the Fe=O bond length was 1.661(3) Å, which closely resembles the **1C-*anti [1.667(9) Å], both Fe(IV)oxo complexes being formed by macrocyclic ligands. Another notable feature is the $Fe\text{-}C_{NHC}$ bond, which in **10B** lies between 1.979(5)-2.045(5) Å, which is almost comparable to **10A** [1.970(2)-2.022(2) Å], but is considerably greater if it is compared to the $Fe\text{-}C_{NHC}$ bond [1.936(4)-1.939(4) Å] of a Fe(II) complex of a macrocyclic ligand consisting of two NHC donors and two pyridine moieties [79]. This observation exemplifies the importance of electronic effects of the specific donor moieties in a macrocyclic ligand. Important structural parameters of Fe(IV)oxo complexes of ligands, **8**, **9** and **10** are tabulated in Table-4.

Conclusion

In this review, the synthetic procedures of the non-heme Fe(IV)oxo complexes have been discussed in detail, among the spectroscopic characterizations, NMR, UV-vis and IR spectroscopic analysis have also been reviewed. This review summarizes the various synthetic strategies adopted by different research groups to successfully obtain the crystal structures of model compounds containing elusive Fe(IV)oxo species. Till date, it has been observed that four different classes of ligands (*e.g.*, macrocyclic TMC-based ligands, pentadentate N5 ligands, tripodal N4 ligands and NHC ligand) discussed in this study formed stable crystal structures, which have been characterized quite extensively. Moreover, it has been observed that the choice of ligand can greatly alter the electronic environment of the metal center, thereby altering the stability of the crystallized Fe(IV)-oxo species. These discussions will provide a clear picture of the methodologies, to be utilized to obtain

TABLE-3
COMPARISON OF STRUCTURAL DATA FOR **4B**, **5B**, **6B** AND **7B** CONTAINING PENTADENTATE N5 LIGANDS

Ligand	Fe(IV)O	$(Fe–L)_{av}$ (Å)	$(Fe–L_{eq})_{av}$ (Å)	$Fe–L_{ax}$ (Å)	Fe=O (Å)	Angle b/w mean equatorial plane of L & Fe=O (°)	*trans*-O/N–Fe=O angle (°)	Ref
4	**4B**	1.972	1.957	2.033(8)	1.639(5)	89.4	179.4(3)	[41]
5	**5B**	2.014	2.004	2.051(2)	1.660(2)	86.9	177.4(8)	[48]
6	**6B**	1.999	1.971	2.115(6)	1.656(4)	88.3	177.0(2)	[50]
7	**7B**	2.053	2.049	2.084(4)	1.677(5)	82.4	170.5(2)	[50]

TABLE-4
COMPARISON OF STRUCTURAL DATA FOR **8B**, **9B** (CONTAINING TRIPODAL N4 LIGAND) AND **10B** (NHC LIGAND)

Ligand	Fe(IV)O	$(Fe–L)_{av}$ (Å)	$(Fe–L_{eq})_{av}$ (Å)	$Fe–L_{ax}$ (Å)	Fe=O (Å)	Angle b/w mean equatorial plane of L & Fe=O (°)	*trans*-O/N–Fe=O angle (°)	Ref
8	**8B**	2.032	2.005	2.112(3)	1.661(2)	89.5	179.3(1)	[44]
9	**9B**	2.007	1.988	2.064(9)	1.680(1)	89.6	179.5(4)	[62]
10	**10B**	2.029	2.010	2.105(4)	1.661(3)	89.4	176.6(2)	[56]

ideal model compounds of iron-containing metalloproteins and help understand the different reaction mechanisms facilitated by these metalloproteins.

CONFLICT OF INTEREST

The authors declare that there is no conflict of interests regarding the publication of this article.

REFERENCES

1. X. Engelmann, I. Monte-Pérez and K. Ray, *Angew. Chem. Int. Ed.*, **55**, 7632 (2016); https://doi.org/10.1002/anie.201600507
2. K. Ray, F.F. Pfaff, B. Wang and W. Nam, *J. Am. Chem. Soc.*, **136**, 13942 (2014); https://doi.org/10.1021/ja507807v
3. K. Ray, F. Heims, M. Schwalbe and W. Nam, *Curr. Opin. Chem. Biol.*, **25**, 159 (2015); https://doi.org/10.1016/j.cbpa.2015.01.014
4. J. Hohenberger, K. Ray and K. Meyer, *Nat. Commun.*, **3**, 720 (2012); https://doi.org/10.1038/ncomms1718
5. C. Krebs, D.P. Galonic-Fujimori, C.T. Walsh and J.M. Bollinger Jr., *Acc. Chem. Res.*, **40**, 484 (2007); https://doi.org/10.1021/ar700066p
6. R.P. Hausinger, *Crit. Rev. Biochem. Mol. Biol.*, **39**, 21 (2004); https://doi.org/10.1080/10409230490440541
7. F.H. Vaillancourt, E. Yeh, D.A. Vosburg, S. Garneau-Tsodikova and C.T. Walsh, *Chem. Rev.*, **106**, 3364 (2006); https://doi.org/10.1021/cr050313i
8. P.M. Wood, *Biochem. J.*, **253**, 287 (1988); https://doi.org/10.1042/bj2530287
9. M. Guo, T. Corona, K. Ray and W. Nam, *ACS Cent. Sci.*, **5**, 13 (2019); https://doi.org/10.1021/acscentsci.8b00698
10. S. Fukuzumi, Y.M. Lee and W. Nam, *ChemCatChem*, **10**, 9 (2018); https://doi.org/10.1002/cctc.201701064
11. W. Zhang, W. Lai and R. Cao, *Chem. Rev.*, **117**, 3717 (2017); https://doi.org/10.1021/acs.chemrev.6b00299
12. F. Nastri, M. Chino, O. Maglio, A. Bhagi-Damodaran, Y. Lu and A. Lombardi, *Chem. Soc. Rev.*, **45**, 5020 (2016); https://doi.org/10.1039/C5CS00923E
13. S. Hematian, I. Garcia-Bosch and K.D. Karlin, *Acc. Chem. Res.*, **48**, 2462 (2015); https://doi.org/10.1021/acs.accounts.5b00265
14. E.L. Hegg and L. Que Jr., *Eur. J. Biochem.*, **250**, 625 (1997); https://doi.org/10.1111/j.1432-1033.1997.t01-1-00625.x
15. C.W. Lee, J.-H. Lee, H. Rimal, H. Park, J.H. Lee and T.-J. Oh, *Int. J. Mol. Sci.*, **17**, 813 (2016); https://doi.org/10.3390/ijms17060813
16. M. Gajhede, D. Schuller, A. Henriksen, T.A. Smith and L.T. Poulos, *Nat. Struct. Mol. Biol.*, **4**, 1032 (1997); https://doi.org/10.1038/nsb1297-1032
17. Y. Yamada, T. Fujiwara, T. Sato, N. Igarashi and N. Tanaka, *Nat. Struct. Biol.*, **9**, 691 (2002); https://doi.org/10.1038/nsb834
18. O. Andreas Andersen, T. Flatmark and E. Hough, *J. Mol. Biol.*, **320**, 1095 (2002); https://doi.org/10.1016/S0022-2836(02)00560-0
19. K. Harlos, C.J. Schofield, Z. Zhang, J. Ren, D.K. Stammers and J.E. Baldwin, *Nat. Struct. Biol.*, **7**, 127 (2000); https://doi.org/10.1038/72398
20. P.L. Roach, I.J. Clifton, C.M. Hensgens, N. Shibata, C.J. Schofield, J. Hajdu and J.E. Baldwin, *Nature*, **387**, 827 (1997); https://doi.org/10.1038/42990
21. E. Carredano, A. Karlsson, B. Kauppi, D. Choudhury, R.E. Parales, J.V. Parales, K. Lee, D.T. Gibson, H. Eklund and S. Ramaswamy, *J. Mol. Biol.*, **296**, 701 (2000); https://doi.org/10.1006/jmbi.1999.3462
22. D.R. Tomchick, P. Phan, M. Cymborowski, W. Minor and T.R. Holman, *Biochemistry*, **40**, 7509 (2001); https://doi.org/10.1021/bi002893d
23. S. Han, L.D. Eltis, K.N. Timmis, S.W. Muchmore and J.T. Bolin, *Science*, **270**, 976 (1995); https://doi.org/10.1126/science.270.5238.976
24. H. Fujii, *Coord. Chem. Rev.*, **226**, 51 (2002); https://doi.org/10.1016/S0010-8545(01)00441-6
25. J.H. Dawson and M. Sono, *Chem. Rev.*, **87**, 1255 (1987); https://doi.org/10.1021/cr00081a015
26. Y. Watanabe and J.T. Groves, Eds.: P.D. Boyer and D.S. Sigman, Molecular Mechanism of Oxygen Activation by Cytochrome P-450, In: The Enzymes, Academic Press: New York, vol. 20, pp. 405-452 (1992).
27. P.R. Ortiz de Montellano, Cytochrome P450, Plenum Press: New York, Ed.: 4 (2015).
28. H.B. Dunford, Heme Peroxidases, Wiley-VCH: New York (1999).
29. H.B. Dunford, Peroxidases and Catalases: Biochemistry, Biophysics, Biotechnology and Physpiology. Wiley, Ed.: 2 (2010).
30. J. Everse, K.E. Everse and M.B. Grisham, Peroxidases in Chemistry and Biology, CRC Press: Boca Raton, Ed.: 1, vol. I & II (1991).
31. J.C. Price, E.W. Barr, B. Tirupati, J.M. Bollinger Jr. and C. Krebs, *Biochemistry*, **42**, 7497 (2003); https://doi.org/10.1021/bi030011f
32. E.I. Solomon, T.C. Brunold, M.I. Davis, J.N. Kemsley, S.K. Lee, N. Lehnert, F. Neese, A.J. Skulan, Y.S. Yang and J. Zhou, *Chem. Rev.*, **100**, 235 (2000); https://doi.org/10.1021/cr9900275
33. E. De Carolis and V. de Luca, *Phytochemistry*, **36**, 1093 (1994); https://doi.org/10.1016/S0031-9422(00)89621-1
34. J.C. Boyington, B.J. Gaffney and L.M. Amzel, *Science*, **260**, 1482 (1993); https://doi.org/10.1126/science.8502991
35. E.I. Solomon, A. Decker and N. Lehnert, *Proc. Natl. Acad. Sci. USA*, **100**, 3589 (2003); https://doi.org/10.1073/pnas.0336792100
36. R.A. Leising, J. Kim, M.A. Perez and L. Que Jr, *J. Am. Chem. Soc.*, **115**, 9524 (1993); https://doi.org/10.1021/ja00074a017
37. C.A. Grapperhaus, B. Mienert, E. Bill, T. Weyhermüller and K. Wieghardt, *Inorg. Chem.*, **39**, 5306 (2000); https://doi.org/10.1021/ic0005238
38. J.U. Rohde, J.H. In, M.H. Lim, W.W. Brennessel, M.R. Bukowski, A. Stubna, E. Münck, W. Nam and L. Que Jr., *Science*, **299**, 1037 (2003); https://doi.org/10.1126/science.299.5609.1037
39. E.K. Barefield and F. Wagner, *Inorg. Chem.*, **12**, 2435 (1973); https://doi.org/10.1021/ic50128a042
40. A. Thibon, J. England, M. Martinho, V.G. Young Jr., J.R. Frisch, R. Guillot, J.J. Girerd, E. Münck, L. Que Jr. and F. Banse, *Angew. Chem. Int. Ed. Engl.*, **47**, 7064 (2008); https://doi.org/10.1002/anie.200801832
41. E.J. Klinker, J. Kaizer, W.W. Brennessel, N.L. Woodrum, C.J. Cramer and L. Que Jr., *Angew. Chem. Int. Ed.*, **44**, 3690 (2005); https://doi.org/10.1002/anie.200500485

42. J. Kaizer, E.J. Klinker, N.Y. Oh, J.U. Rohde, W.J. Song, A. Stubna, J. Kim, E. Münck, W. Nam and L. Que Jr., *J. Am. Chem. Soc.*, **126**, 472 (2004); https://doi.org/10.1021/ja037288n
43. M. Lubben, A. Meetsma, E.C. Wilkinson, B. Feringa and L. Que Jr., *Angew. Chem. Int. Ed. Engl.*, **34**, 1512 (1995); https://doi.org/10.1002/anie.199515121
44. J. England, Y. Guo, E.R. Farquhar, V.G. Young Jr., E. Mu¨nck and L. Que Jr., *J. Am. Chem. Soc.*, **132**, 8635 (2010); https://doi.org/10.1021/ja100366c
45. J.A. Halfen and V.G. Young Jr., *Chem. Commun.*, 2894 (2003); https://doi.org/10.1039/b311520h
46. C. Bucher, G. Royal, J.-M. Barbe and R. Guilard, *Tetrahedron Lett.*, **40**, 2315 (1999); https://doi.org/10.1016/S0040-4039(99)00190-2
47. S. Sahu, M.G. Quesne, C.G. Davies, M. Dürr, I. Ivanovic-Burmazovic, M.A. Siegler, G.N.L. Jameson, S.P. de Visser and D.P. Goldberg, *J. Am. Chem. Soc.*, **136**, 13542 (2014); https://doi.org/10.1021/ja507346t
48. S. Sahu, B. Zhang, C.J. Pollock, M. Dürr, C.G. Davies, A.M. Confer, I. Ivanovic-Burmazovic, M.A. Siegler, G.N. Jameson, C. Krebs and D.P. Goldberg, *J. Am. Chem. Soc.*, **138**, 12791 (2016); https://doi.org/10.1021/jacs.6b03346
49. M. Mitra, H. Nimir, S. Demeshko, S.S. Bhat, S.O. Malinkin, M. Haukka, J. Lloret-Fillol, G.C. Lisensky, F. Meyer, A.A. Shteinman, W.R. Browne, D.A. Hrovat, M.G. Richmond, M. Costas and E. Nordlander, *Inorg. Chem.*, **54**, 7152 (2015); https://doi.org/10.1021/ic5029564
50. W. Rasheed, A. Draksharapu, S. Banerjee, V.G. Young Jr., R. Fan, Y. Guo, M. Ozerov, J. Nehrkorn, J. Krzystek, J. Telser and L. Que Jr, *Angew. Chem. Int. Ed.*, **130**, 9531 (2018); https://doi.org/10.1002/ange.201804836
51. H. Wittmann, V. Raab, A. Schorm, J. Plackmeyer and J. Sundermeyer, *Eur. J. Inorg. Chem.*, **2001**, 1937 (2001); https://doi.org/10.1002/1099-0682(200108)2001:8<1937::AID-EJIC1937>3.0.CO;2-I
52. M.P. Lanci, V.V. Smirnov, E.V. Gauchenova, J. Sundermeyer, C.J. Cramer and J.P. Roth, *J. Am. Chem. Soc.*, **129**, 14697 (2007); https://doi.org/10.1021/ja074620c
53. R.H. Holm, P. Kennepohl and E.I. Solomon, *Chem. Rev.*, **96**, 2239 (1996); https://doi.org/10.1021/cr9500390
54. Y. Lu and J.S. Valentine, *Curr. Opin. Struct. Biol.*, **7**, 495 (1997); https://doi.org/10.1016/S0959-440X(97)80112-1
55. R. César, A. Marta, M. Mercedes, W. Volker, M.M. Luisa, A. Victoria, C.M. Cruz and R.M. Joaquín, *Chem. Lett.*, **24**, 759 (1995); https://doi.org/10.1246/cl.1995.759
56. S. Meyer, I. Klawitter, S. Demeshko, E. Bill and F. Meyer, *Angew. Chem. Int. Ed. Engl.*, **52**, 901 (2013); https://doi.org/10.1002/anie.201208044
57. H.M. Bass, S.A. Cramer, J.L. Price and D.M. Jenkins, *Organometallics*, **29**, 3235 (2010); https://doi.org/10.1021/om100625g
58. E. Diez-Barra, A. De la Hoz, A. Sanchez-Migallon and J. Tejeda, *Heterocycles*, **34**, 1365 (1992); https://doi.org/10.3987/COM-92-6024
59. J. Prakash, G.T. Rohde, K.K. Meier, E. Münck and L. Que Jr., *Inorg. Chem.*, **54**, 11055 (2015); https://doi.org/10.1021/acs.inorgchem.5b02011
60. S. Schaub, A. Miska, J. Becker, S. Zahn, D. Mollenhauer, S. Sakshath, V. Schünemann and S. Schindler, *Angew. Chem. Int. Ed. Engl.*, **57**, 5355 (2018); https://doi.org/10.1002/anie.201800475
61. J. England, J.O. Bigelow, K.M. Van Heuvelen, E.R. Farquhar, M. Martinho, K.K. Meier, J.R. Frisch, E. Münck and L. Que, *Chem. Sci.*, **5**, 1204 (2014); https://doi.org/10.1039/C3SC52755G
62. D.C. Lacy, R. Gupta, K.L. Stone, J. Greaves, J. Ziller, M.P. Hendrich and A.S. Borovik, *J. Am. Chem. Soc.*, **132**, 12188 (2010); https://doi.org/10.1021/ja1047818
63. O. Pestovsky, S. Stoian, E.L. Bominaar, X. Shan, E. Münck, L. Que and A. Bakac, *Angew. Chem.*, **117**, 7031 (2005); https://doi.org/10.1002/ange.200502686
64. T.A. Jackson, J.-U. Rohde, M.S. Seo, C.V. Sastri, R. DeHont, A. Stubna, T. Ohta, T. Kitagawa, E. Münck, W. Nam and L. Que, *J. Am. Chem. Soc.*, **130**, 12394 (2008); https://doi.org/10.1021/ja8022576
65. D.-H. Chin, A.L. Balch and G.N. La Mar, *J. Am. Chem. Soc.*, **102**, 1446 (1980); https://doi.org/10.1021/ja00524a051
66. S.O. Kim, C.V. Sastri, M.S. Seo, J. Kim and W. Nam, *J. Am. Chem. Soc.*, **127**, 4178 (2005); https://doi.org/10.1021/ja043083i
67. J.E. Penner-Hahn, K. Smith Eble, T.J. McMurry, M. Renner, A.L. Balch, J.T. Groves, J.H. Dawson and K.O. Hodgson, *J. Am. Chem. Soc.*, **108**, 7819 (1986); https://doi.org/10.1021/ja00284a054
68. T. Wolter, W. Meyer-Klaucke, M. Müther, D. Mandon, H. Winkler, A. X. Trautwein and R. Weiss, *J. Inorg. Biochem.*, **78**, 117 (2000); https://doi.org/10.1016/S0162-0134(99)00217-2
69. C.J. Reed and T. Agapie, *J. Am. Chem. Soc.*, **141**, 9479 (2019); https://doi.org/10.1021/jacs.9b03157
70. C.E. MacBeth, A.P. Golombek, V.G. Young Jr., C. Yang, K. Kuczera, M.P. Hendrich and A.S. Borovik, *Science*, **289**, 938 (2000); https://doi.org/10.1126/science.289.5481.938
71. E.M. Matson, Y.J. Park and A.R. Fout, *J. Am. Chem. Soc.*, **136**, 17398 (2014); https://doi.org/10.1021/ja510615p
72. Y. Zang, Y. Dong, L. Que Jr., K. Kauffmann and E. Muenck, *J. Am. Chem. Soc.*, **117**, 1169 (1995); https://doi.org/10.1021/ja00108a050.
73. G. Xue, D. Wang, R. De Hont, A.T. Fiedler, X. Shan, E. Münck and L. Que Jr., *Proc. Natl. Acad. Sci. USA*, **104**, 20713 (2007); https://doi.org/10.1073/pnas.0708516105
74. H.-F. Hsu, Y. Dong, L. Shu, V.G. Young Jr. and L. Que Jr., *J. Am. Chem. Soc.*, **121**, 5230 (1999); https://doi.org/10.1021/ja983666q
75. A. Ghosh, F.T. de Oliveira, T. Yano, T. Nishioka, E.S. Beach, I. Kinoshita, E. Münck, A.D. Ryabov, C.P. Horwitz and T.J. Collins, *J. Am. Chem. Soc.*, **127**, 2505 (2005); https://doi.org/10.1021/ja0460458
76. K. Ray, J. England, A.T. Fiedler, M. Martinho, E. Münck and L. Que Jr., *Angew. Chem. Int. Ed.*, **47**, 8068 (2008); https://doi.org/10.1002/anie.200802219
77. L.G. Wade, Organic Chemistry, Pearson Prentice Hall: NJ, Ed.: 8 (2006).
78. F.A. Carey, Organic Chemistry. McGraw Hill: New York, Ed.: 6 (2006).
79. I. Klawitter, M.R. Anneser, S. Dechert, S. Demeshko, S. Haslinger, S. Meyer, A. Pöthig, F.E. Kühn and F. Meyer, *Organometallics*, **34**, 2819 (2015); https://doi.org/10.1021/acs.organomet.5b00103